國 立 交 通 大 學

電信工程學系

碩 士 論 文

近接頻率訊號之參數估測

Parameter estimation of two closely spaced
frequency signals

研究生：涂志帆

指導教授：高銘盛教授

中 華 民 國 九十八 年 六 月

近接頻率訊號之參數估測

Parameter Estimation of two closely spaced frequency signals

研 究 生：涂志帆　　　　　Student: Zhi-Fan Tu

指導教授：高銘盛　　　　　Advisor: Ming-Seng Kao

國 立 交 通 大 學

電 信 工 程 學 系

碩 士 論 文

A Thesis

Submitted to Department of Communication Engineering

College of Electrical and Computer Engineering

National Chiao Tung University

in partial Fulfillment of the Requirements

for the Degree of

Master of Science

in

Communication Engineering

June 2009

Hsinchu, Taiwan, Republic of China

中 華 民 國 九 十 八 年 六 月

近接頻率訊號之參數估測

研究生：涂志帆　　　　　　　　指導教授：高銘盛 教授

國立交通大學

電信工程學系碩士班

摘　要

此篇論文呈現一個演算法以估測二個頻率非常接近之弦波訊號的參數。由於此波訊號之頻率太靠近，以致於很難使用濾波器分別濾出其中之一。我們的方法是設計一種特別的取樣方式來達成零干擾，並且運用統計之概念估測訊號中振幅和相位的變化。此方法架構於簡單的取樣技術，故可降低接收器之複雜度。此技術可運用於遙感系統和雷達系統，藉此可以有效偵測信號頻率和相位的訊息。

Parameter estimation of two closely spaced frequency signals

Student: Zhi-Fan Tu   Advisor: Prof. Ming-Seng Kao

Department of Communication Engineering
National Chiao Tung University

Abstract

This paper presents an algorithm to estimate the parameters of two closely spaced sinusoid signals. Since the frequencies of two sinusoid signals are very close, it is difficult to separate them with filtering. Our approach is to design a special sampling method to achieve zero interference under ideal conditions, and estimate the variations of amplitude and phase with statistic approach. It is based on a simple sampling technique, which can reduce the complexity of detection receiver. The algorithm can be applied to remote sensing system and radar system, in order to detect the desired amplitude and phase information.

Acknowledgements

I would like to show my deepest appreciation to my advisor, Dr. Ming-Seng Kao, for his enthusiastic guidance and patience. And I would to thanks my parents for raising and cultivating me. Besides, I would like to thanks all the members in Damily for their support, especially ZePhoen,Kong and SinoPhoen,Su. Their teachings give me a lot of directions of my life during the three years. All of their selfless love and support are the strongest energy for me. Without their encouragement, this work could not be possible. Finally, I would like to show my sincere thanks to our heaven Father and Mother for their invaluable love.

Table of Contents

List of Figures

Chapter 1

Introduction

1.1 Problem description
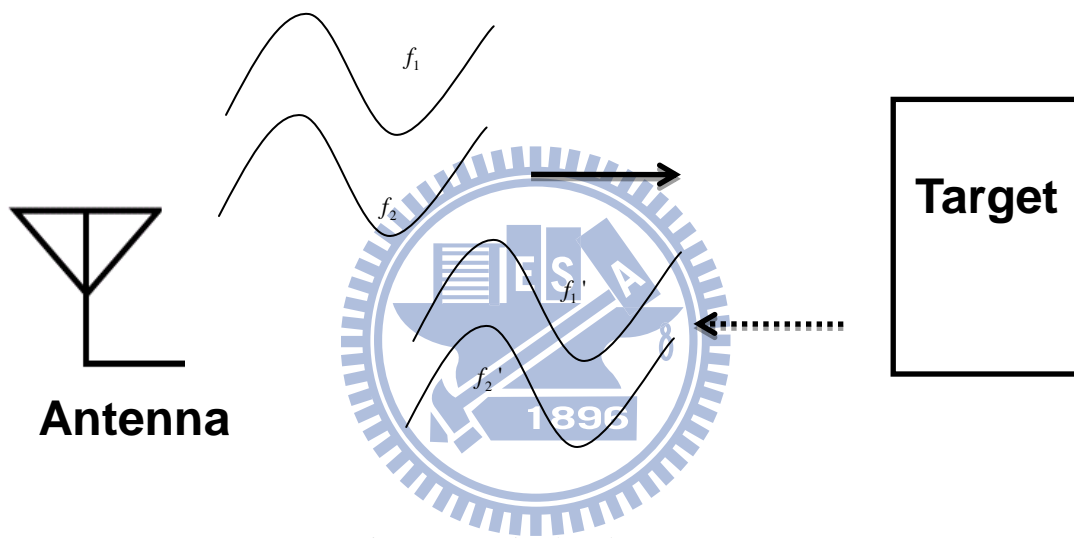
Figure 1.1: A simple radar system

This paper deals with a sinusoidal estimation problem as shown in Figure 1.1, where the antenna transmits and receives a special signal consisting of two frequencies. The signal is superimposed, including two closely space frequency sinusoids. The frequency of two signals is too close to be separated with filtering. Moreover, the frequency of two signals may vary on reflecting from the target as a result of Doppler effect when the target is moving. Our aim is to detect the phase and amplitude variations of both signals. By this information we can estimate distance, position and velocity of the target accurately.

Currently, a popular approach for resolving this problem is to employ an information theoretic criterion, such as the Minimum Description Length (MDL) rule [1,2]. However, the results obtained by these methods are not satisfactory, and the computational cost for

implementing them is considerably high. Other methods are derived from the maximum likelihood function [3-6]. Although they show excellent performance but unfortunately are computationally intensive too. In this paper, we develop a new strategy to estimate the parameters of two sinusoids. Our method is based on a simple sampling technique and statistic concepts, which can reduce the complexity of parameter estimation.

The paper is organized as follows. The derivation of the detection algorithm is given in Chapter 2. In Chapter 3 we present performance analysis and simulation results of the algorithm. Finally, the conclusion is given in Chapter 4.
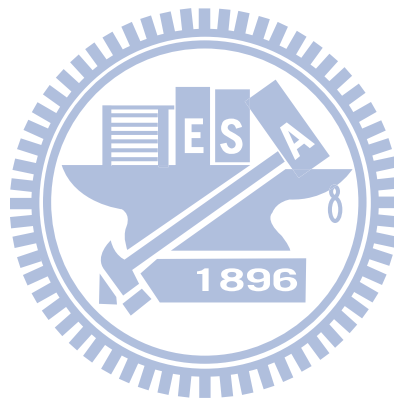
Chapter 2

Detection Algorithm

In this chapter, we will describe the proposed detection algorithm of two signals. Both amplitude and phase variations will be estimated in our detection algorithm. In the following, detection of $s_2(t)$ is described first, and then detection of $s_1(t)$ is given next.

Consider two desired signals given as

$$s_1(t) = A_1 \cos(w_1 t + \phi_1) \tag{2.1}$$
$$s_2(t) = A_2 \cos(w_2 t + \phi_2) \tag{2.2}$$

and for a radar system the received signal is

$$r(t) = s_1(t) + s_2(t) + n(t)$$
$$= A_1 \cos(w_1 t + \phi_1) + A_2 \cos(w_2 t + \phi_2) + n(t) \tag{2.3}$$

where $n(t)$ is the noise. The information we want to detect is the phase and amplitude variations of $s_1(t)$ and $s_2(t)$. Since the two frequencies w_1 and w_2 are very close, it is difficult to separate the two signals with filtering. For simplicity, we assume $n(t) = 0$ in the following analysis and will include it later.

2.1 Detection of $s_2(t)$

In order to detect $s_2(t)$, we must eliminate the interference coming from $s_1(t)$. We will achieve the aim with a special sampling technique . Let the sampling interval be

chose as

$$t_s = (m + \frac{1}{N})T_1 \quad , \tag{2.4}$$

where T_1 is the period of $s_1(t)$, while m, N are integers and $m \geq 0, N \geq 2$.

The received signal $r(t)$ is sampled at $t = kt_s, k = 0,1,2,...N-1$. The *kth* sample of $r(t)$ is

$$r(k) = r(kt_s) = s_1(k) + s_2(k)$$

where

$$s_1(k) = s_1(kt_s) = A_1 \cos[2\pi f_1 k(m + \frac{1}{N})T_1 + \phi_1]$$

$$= A_1 \cos[2\pi(km + \frac{k}{N}) + \phi_1] = A_1 \cos(2\pi \frac{k}{N} + \phi_1) \tag{2.5}$$

From trigonometry, it can be proved:

$$\sum_{k=0}^{N-1} cos(\frac{2\pi}{N}k + \phi_1) = 0 \quad , \qquad N \geq 2 \tag{2.6}$$

for any ϕ_1. The reasoning behind Eq. (2.6) is sample. We can look cosine function as a unit circle and sample at circumference, as shown in Figure 2.1, and then the sum of x axis values of all samples vanishes.
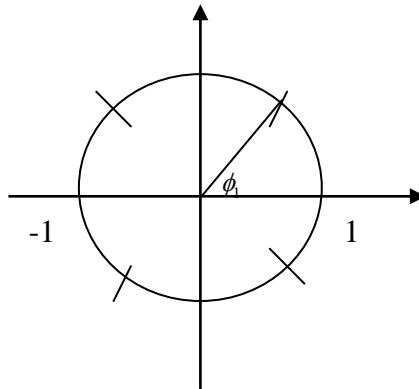
Figure 2.1: Concept of sampling technique.

From Eqs. (2.5) and (2.6), we obtain

$$\sum_{k=0}^{N-1} s_1(k) = A_1 \cdot \sum_{k=0}^{N-1} cos(\frac{2\pi}{N}k + \phi_1) = 0 \quad , \quad \text{for any} \quad \phi_1 \qquad (2.7)$$

Note that Eq. (2.7) is independent of ϕ_1, indicating that we can achieve zero interference coming from $s_1(t)$ if t_s is taken as Eq. (2.4).

Next we consider the relationship between t_s and T_2, where T_2 is the period of $s_2(t)$. Let the sampling interval be

$$t_s = \alpha \cdot T_2 \quad . \qquad (2.8)$$

where α is an integer.

Then the sampled value of $s_2(t)$ is written as

$$s_2(k) = s_2(kt_s) = A_2 \cdot cos(2\pi f_2 k\alpha T_2 + \phi_2) = A_2 \cdot cos\phi_2 \qquad (2.9)$$

In Eqs. (2.4) and (2.8), the sampling interval should be the same, thus we obtain

$$\alpha T_2 = (m + \frac{1}{N})T_1 \quad \Rightarrow \quad \frac{w_1}{w_2} = \frac{mN+1}{\alpha N} \qquad (2.10)$$

Eq.(2.10) is the requirement to optimally detect $s_2(t)$ while completely eliminate the interference of $s_1(t)$. To optimally detect $s_2(t)$ without the interference of $s_1(t)$, Eq.(2.10) should be satisfied. In practice we can design the frequencies of $s_1(t)$ and $s_2(t)$ such that Eq. (2.8) is satisfied for some set of (α, N, m).

If we set $\alpha = m$ then Eq. (2.10) becomes

$$\frac{w_1}{w_2} = 1 + \frac{1}{\alpha N} \quad . \tag{2.11}$$

Thus the frequencies (w_1, w_2) can be very close with a large αN.

Consider an observation interval (T_{ob}) consisting of M time blocks, given as

$$T_{ob} = M \cdot T_p \tag{2.12}$$

and

$$T_p = N t_s + \tau \tag{2.13}$$

where τ is a fixed time delay and $\tau \leq t_s$. Assume $s_2(t)$ slowly varies with time such that its phase and amplitude keeps constant within T_{ob}. Here we use a non-uniform sampling scheme. In the first time block, i.e., $0 \leq t \leq T_p$, we take N samples at $t = k t_s$, $k=0,1,2,...,N-1$, and take zero samples within $N t_s \leq t \leq T_p$. From Eqs. (2.7) and (2.9), the average value of these N samples is written as

$$x_0 = \frac{1}{N} \sum_{k=0}^{N-1} r(k) = \frac{1}{N} \sum_{k=0}^{N-1} [s_1(k) + s_2(k)] = A_2 \cos \phi_2 \quad , \tag{2.14}$$

where ϕ_2 is the phase of $s_2(t)$ at t=0.

Next consider the time interval $T_p \leq t \leq 2T_p$. Again we take N samples at $t = T_p + j t_s$, $j=0,1,2,...,N-1$, and have zero samples within $T_p + N t_s \leq t \leq 2T_p$. In this case the sampled signal is written as

$$\begin{aligned}
r(j) &= r(T_p + j t_s) \\
&= A_1 \cos[w_1(T_p + j t_s) + \phi_1] + A_2 \cos[w_2(T_p + j t_s) + \phi_2] \\
&= A_1 \cos[w_1(N t_s + j t_s + \tau) + \phi_1] + A_2 \cos[w_2(N t_s + j t_s + \tau) + \phi_2]
\end{aligned} \tag{2.15}$$

Using Eqs. (2.4) and (2.8), we can reformulate Eq. (2.15) as

$$r(j) = A_1 \cos(\frac{2\pi}{N}j + w_1\tau + \phi_1) + A_2 \cos(w_2\tau + \phi_2) \ . \qquad (2.16)$$

Since

$$\sum_{j=0}^{N-1} \cos(\frac{2\pi}{N}j + w_1\tau + \phi_1) = 0 \qquad (2.17)$$

for any $w_1\tau + \phi_1$, the average value of $r(j)$, $j=0,1,2,...,N-1$, is given as

$$x_1 = \frac{1}{N}\sum_{j=0}^{N-1} r(j) = A_2 \cos(w_2\tau + \phi_2) \ . \qquad (2.18)$$

In general, we will obtain the average for the time block $iT_p \le t \le (i+1)T_p$ as

$$x_i = A_2 \cos[w_2(i\tau) + \phi_2] \ . \qquad (2.19)$$

If we take

$$\tau = \frac{T_2}{M} \qquad (2.20)$$

Then, Eq. (2.19) becomes

$$x_i = A_2 \cos(2\pi\frac{i}{M} + \phi_2) \qquad (2.21)$$

When M is large, from Eq. (2.21) we can look $(x_0, x_1,..., x_{M-1})$ as the sampled values of a slow-varying sinusoid whose frequency is 1/M, with amplitude A_2 and phase ϕ_2. Note that A_2 and ϕ_2 are the amplitude and phase of $s_2(t)$ too. Apparently, we can obtain the information of A_2 and ϕ_2 from the set of samples $(x_0, x_1,..., x_{M-1})$.

For a sinusoid we have

$$\frac{1}{T} \int_0^T [A\cos(wt + \theta)]^2 dt = \frac{A^2}{2} \quad . \tag{2.22}$$

Mathematically, we have the following approximations when M is large:

$$\frac{1}{M} \cdot \sum_{i=0}^{M-1} x_i^2 \approx \frac{1}{T} \int_0^T [A\cos(2\pi\frac{i}{M} + \phi_2)]^2 dt$$

$$\Rightarrow \frac{1}{M} \cdot \sum_{i=0}^{M-1} x_i^2 \approx \frac{A^2}{2} \tag{2.23}$$

Hence, we can estimate A$_2$ as

$$\hat{A}_2 \approx \sqrt{\frac{2}{M} \cdot \sum_{i=0}^{M-1} x_i^2} \quad . \tag{2.24}$$

From previous results, a set of parameters $(x_0, x_1,...,x_{M-1})$ is obtained within the time interval T_{ob}, which reveals the amplitude of $s_2(t)$ during this period. Let the total observation time be $T_{total} = qT_{ob}$ and $q \gg 1$. Under this circumstance we can obtain q sets of parameters, $(x_{i,0}, x_{i,1},...,x_{i,M-1})$, $i = 0,1,2,..q-1$, where $(x_{i,0}, x_{i,1},...,x_{i,M-1})$ is obtained in the time interval $iT_{ob} \le t \le (i+1)T_{ob}$.

Let $\phi_{2,k}$ be the phase of $s_2(t)$ at $t = kT_{ob}$ and $A_{2,k}$ be the amplitude, and assume they are constants during the time interval $kT_{ob} \le t \le (k+1)T_{ob}$. We can estimate $A_{2,k}$ with the method just derived. As a consequence, we will obtain a set of estimated amplitudes $(A_{2,0}, A_{2,1},..., A_{2,q-1})$. The sets of data $\hat{A}_{2,k}$ will be used to evaluate the phase variations of $s_2(t)$. The figure below explains the method.
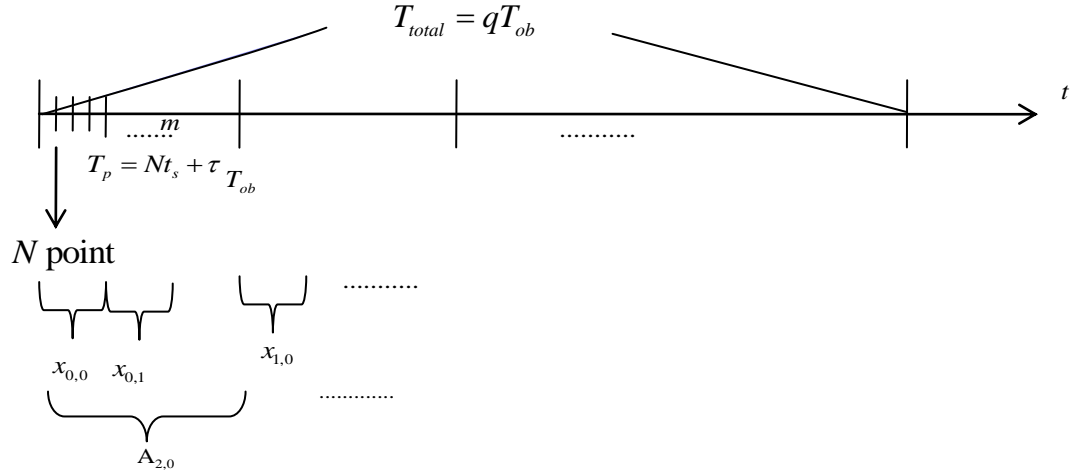
Figure 2.2: Statistic concepts of the algorithm.

Using the fact that

$$\frac{1}{T}\int_0^T [A\cos(wt+\Delta\phi)-A'\cos wt]^2 \, dt = \frac{1}{T}\left\{ T \bullet \left[\frac{A^2+A'^2}{2} - AA'\cos\Delta\phi \right] \right\}$$
$$= \frac{A^2+A'^2}{2} - AA'\cos\Delta\phi \tag{2.25}$$

Thus if the integration is available, the phase shift is calculated as

$$\Delta\phi = \cos^{-1}\left(\frac{\dfrac{A^2+A'^2}{2} - \dfrac{1}{T}\int_0^T [A\cos(wt+\Delta\phi)-A'\cos wt]^2 \, dt}{AA'} \right) \tag{2.26}$$

Based on the relationship of Eq. (2.26), we can define the phase shift between kT_{ob} and $(k+1)T_{ob}$ as

$$\Delta\phi_{k,k+1} = \cos^{-1}\left\{ \frac{1}{A_{2,k}\cdot A_{2,k+1}}\left[\frac{A_{2,k}^2+A_{2,k+1}^2}{2} - \frac{1}{M}\sum_{i=0}^{M-1}(x_{k,i}-x_{k+1,i})^2 \right] \right\} \tag{2.27}$$

Consequently, we can calculate phase variation of $s_2(t)$ from Eq. (2.27).

9

2.2 Detection of $s_1(t)$

We had derived the method to detect the phase and amplitude of $s_2(t)$ without the interference coming from $s_1(t)$. The same idea can be applied to detect the phase and amplitude variations of $s_1(t)$ without the interference coming from $s_2(t)$. Let t_s' be the sampling frequency to be used to detect $s_1(t)$ and assume

$$t_s' = \beta \cdot T_1 \qquad (2.28)$$

where β is an integer.

Then the sampled value of $s_1(t)$ is written as

$$s_1(k) = s_1(kt_s') = A_1 \cdot \cos(2\pi f_1 k \beta T_1 + \phi_2) = A_1 \cdot \cos\phi_1 \quad , \qquad (2.29)$$

Consider the samples of $s_2(t)$. Let the sampling interval be chosen as

$$t_s' = (l + \frac{h}{W})T_2 \quad , \qquad (2.30)$$

where l, W, h are integers and (W, h) are relative prime numbers . In this case we have

$$
\begin{aligned}
s_2(k) = s_2(kt_s') &= A_2 \cos[2\pi f_2 k(l + \frac{h}{W})T_2 + \phi_2] \\
&= A_2 \cos[2\pi(kl + k\frac{h}{W}) + \phi_2] = A_2 \cos(2\pi k \frac{h}{W} + \phi_2)
\end{aligned}
\qquad (2.31)
$$

It can be proved:

$$\sum_{k=0}^{W-1} s_2(k) = A_2 \cdot \sum_{k=0}^{W-1} \cos(2\pi k \frac{h}{W} + \phi_2) = 0 \qquad , \text{ for any } \phi_2 \qquad (2.32)$$

Note that Eq. (2.32) is independent of ϕ_2 , indicating that we can achieve zero interference coming from $s_2(t)$.

From Eqs. (2.28) and (2.30), we obtain

$$\beta T_1 = (l + \frac{h}{W})T_2 \quad \Rightarrow \quad \frac{w_1}{w_2} = \frac{\beta W}{l \cdot W + h} \quad . \tag{2.33}$$

Eq. (2.33) is the requirement to optimally detect $s_1(t)$ while completely eliminate the interference of $s_2(t)$. In practice we can design the frequencies of $s_1(t)$ and $s_2(t)$ such that the equality of Eq. (2.33) is satisfied for some parameters (l, W, β, h). From Eqs. (2.11) and (2.33), we can obtain

$$\frac{w_1}{w_2} = 1 + \frac{1}{\alpha N} = \frac{\beta W}{l \cdot W + h} \quad . \tag{2.34}$$

Thus

$$(\beta W \,)(\alpha N \,) = (\alpha N + \, 1 \,)(\, W + \tag{2.35}$$

Let

$$\begin{cases} \beta W = \alpha N + 1 \\ \alpha N = l \cdot W + h \end{cases} \Rightarrow \beta W = l \cdot W + h + 1 \tag{2.36}$$

We can choose

$$\begin{cases} \beta = l + 1 \\ h = W - 1 \end{cases} \tag{2.37}$$

Eq. (2.37) is the relationship between the parameters (l, W, β, h), which satisfies the requirement that (W, h) are relative prime numbers.

Consider an observation interval ($T_{ob}{}'$) consisting of M time blocks, given as

$$T_{ob}{}' = M \cdot T_p{}' \tag{2.38}$$

and

$$T_p' = Wt_s' + \tau' \qquad (2.39)$$

where τ' is a fixed time delay and $\tau' \leq t_s'$. Assume $s_1(t)$ slowly varies with time such that its phase and amplitude keeps constant within T_{ob}'. Thus, we use a non-uniform sampling scheme. In the first time block, i.e., $0 \leq t \leq T_p'$, we take W samples at $t = kt_s'$, $k=0,1,2,...,W-1$, and take zero samples within $Wt_s' \leq t \leq T_p'$. From Eq. (29) and (32), the average value of these W samples is written as

$$y_0 = \frac{1}{W} \sum_{k=0}^{W-1} r(k) = \frac{1}{W} \sum_{k=0}^{W-1} [s_1(k) + s_2(k)] = A_1 \cos \phi_1 \quad , \qquad (2.40)$$

where ϕ_1 is the phase of $s_1(t)$ at t=0.

Next consider the time interval $T_p' \leq t \leq 2T_p'$. Again we take W samples at $t = T_p' + jt_s'$, $j=0,1,2,...,W-1,$ and have zero samples within $T_p' + Wt_s' \leq t \leq 2T_p'$. In this case the sampled signal is written as

$$\begin{aligned} r(j) &= r(T_p' + jt_s') \\ &= A_1 \cos[w_1(T_p' + jt_s' + \phi_1] + A_2 \cos[w_2(T_p' + jt_s') + \phi_2] \\ &= A_1 \cos[w_1(Wt_s' + jt_s' + \tau') + \phi_1] + A_2 \cos[w_2(Wt_s' + jt_s' + \tau') + \phi_2] \end{aligned} \qquad . \qquad (2.41)$$

Using Eq. (2.28) and (2.30), we can reformulate Eq. (2.41) as

$$r(j) = A_1 \cos(w_1\tau' + \phi_1) + A_2 \cos(2\pi j \frac{h}{W} + w_2\tau' + \phi_2) \quad . \qquad (2.42)$$

Since

$$\sum_{j=0}^{W-1} \cos(2\pi j \frac{h}{W} + w_2\tau' + \phi_2) = 0 \qquad (2.43)$$

for any $w_2\tau'+\phi_2$, the average value of $r(j)$, $j=0,1,2,...,W-1$, is given as

$$y_1 = \frac{1}{W}\sum_{j=0}^{W-1} r(j) = A_1\cos(w_1\tau'+\phi_1) \quad . \tag{2.44}$$

In general, we will obtain the average for the time block $iT_p' \leq t \leq (i+1)T_p'$ as

$$y_i = A_1\cos[w_1(i\tau)+\phi_1] \quad , \tag{2.45}$$

If we take

$$\tau' = \frac{T_1}{M} \quad , \tag{2.46}$$

then

$$y_i = A_1\cos(2\pi\frac{i}{M}+\phi_1) \tag{2.47}$$

When M is large, from Eq. (2.47) we can look $(y_0, y_1,...,y_{M-1})$ as the sampled values of a slow-varying sinusoid whose frequency is 1/M, with amplitude A_1 and phase ϕ_1 of $s_1(t)$.

From Eqs. (2.21) and (2.22), we can estimate A₁ as

$$\hat{A}_1 = \sqrt{\frac{2}{M}\cdot\sum_{i=0}^{M-1} y_i^2} \quad . \tag{2.48}$$

From previous results, a set of parameters $(y_0, y_1,..., y_{M-1})$ is obtained within the time interval T_{ob}', which reveals the amplitude of $s_1(t)$ during this period. Let the total observation time be $T_{total}' = qT_{ob}'$ and $q \gg 1$. Under this circumstance we can obtain q sets of parameters, $(y_{i,0}, y_{i,1},..., y_{i,M-1})$, $i=0,1,2,..q-1$, where $(y_{i,0}, y_{i,1},..., y_{i,M-1})$ is obtained in the time interval $iT_{ob}' \leq t \leq (i+1)T_{ob}'$. Let $\phi_{1,k}$ be the phase of $s_1(t)$ at $t=kT_{ob}'$ and $A_{1,k}$ be the amplitude, and assume they are constants during the time interval $kT_{ob}' \leq t \leq (k+1)T_{ob}'$.

We can estimate $A_{1,k}$ with the method just derived. As a consequence, we will obtain a set of estimated amplitudes $(A_{1,0}, A_{1,1}, ..., A_{1,q-1})$. The sets of data $\hat{A}_{1,k}$ will be used to evaluate the phase variations of $s_1(t)$.

Based on the relationship of Eq. (2.26), we also can define the phase shift of $s_1(t)$ between kT_{ob}' and $(k+1)T_{ob}'$ as

$$\Delta\phi_{k,k+1} = \cos^{-1}\left\{\frac{1}{A_{1,k} \cdot A_{1,k+1}}\left[\frac{A_{1,k}^2 + A_{1,k+1}^2}{2} - \frac{1}{M}\sum_{i=0}^{M-1}(y_{k,i} - y_{k+1,i})^2\right]\right\} \qquad (2.49)$$

Consequently, we can calculate phase variation of $s_1(t)$ from Eq. (2.49).
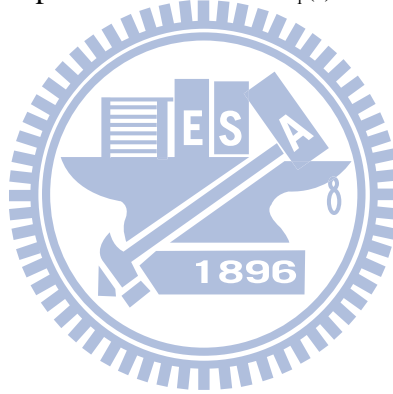
2.3 Simulation Results

2.3.1 Simulation results with detection of $s_2(t)$

In this section we will use computer simulation results to verify accuracy of the detection algorithm. First, we set the parameters used in simulation as the table below:

Tab. 2.1: System Parameters for the Simulation of Detection Algorithm for $s_2(t)$.

Number of samples	N =203
$\alpha = m$	3
Phase of $s_1(t)$	$\phi_1 = 33°$
Phase of $s_2(t)$	$\phi_2 = 27°$
Frequency of $s_1(t)$	$f_1 = 610\ MHz$
Frequency of $s_2(t)$	$f_2 = 609\ MHz$
Sample interval	$t_s = 4.9261\ ns$
Time blocks	$T_p = 1.0001\ \mu s$
Number of T_p	M =20
Time delay	$\tau = 0.082102\ ns$
Observation interval	$T_{ob} = 20.002\ \mu s$
Number of T_{ob}	q =20

Note that the parameters given above satisfy Eqs. (2.10) and (2.20), and the difference of two sinusoid frequencies is 1 MHz. After setting the parameters, we define the Amplitude Error Ratio as

$$E_{A_i} = \frac{\frac{1}{q}\sum_{k=0}^{q-1} \left|\hat{A}_{i,\,k} - A\right|_i}{A_i} \qquad , \text{i} = 1 \text{ or } 2. \qquad (2.50)$$

where $\hat{A}_{i,k}$ is the estimated amplitude while A_i is the actual amplitude. And the Phase Shift Error Ratio as

$$E_{\Delta\phi_i} = \frac{\frac{1}{q-1}\sum_{k=0}^{q-2} \left|\Delta\hat{\phi}_{i,k} - \Delta\phi_i\right|}{\Delta\phi_i} \qquad , \text{i} = 1 \text{ or } 2. \qquad (2.51)$$

where $\Delta\hat{\phi}_{i,k}$ is the estimated phase shift while $\Delta\phi_i$ is the actual phase shift.

Figure 2.3 and Figure 2.4 show the simulation results under different A_2/A_1 ratio, where Amplitude Error Ratio is very small between $10^{-10} \sim 10^{-11}$. It reveals that our detection algorithm works accurately.
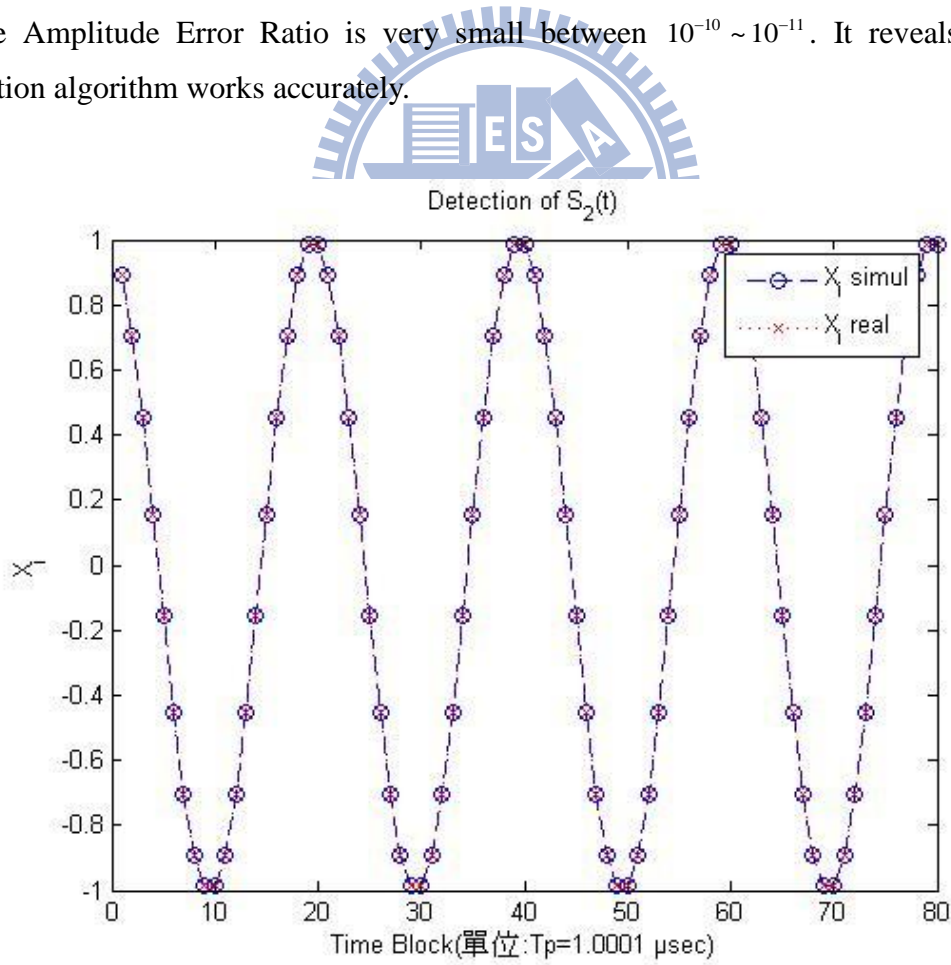

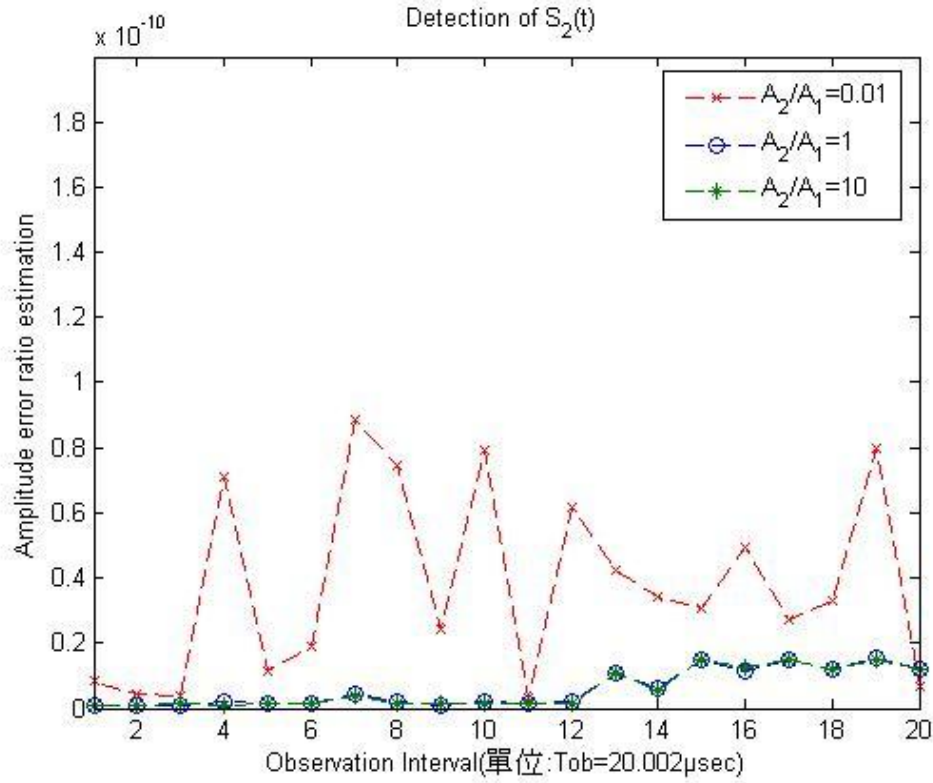Figure 2.3: The average sampled values of output Xi when $A_1 = A_2 = 1$.

Figure 2.4: Amplitude Error Ratio under different A_2 / A_1.

Because the radar system receives the signal reflecting from the target, therefore A_2, amplitude of $s_2(t)$, may vary slowly with time in practice. Thus, we assume $A_2(t)$ is an exponential function

$$A_2(t) = A_2 \cdot (1 + e^{-p\frac{t}{T}}) \tag{2.52}$$

where p and T are constants. We set $A_1 = A_2 = 10$, p=0.07, 0.1 ,0.5 , and T=4x10^{-5} s where the variables p and T decide the decay of the amplitude variation. The average sampled values of output with amplitude variation are shown in Figure 2.5. Figure 2.6 shows the Amplitude Error Ratio of $A_2(t)$ with different p. The amplitude varies faster when p is large. Thus the Amplitude Error Ratio increases in the earlier observation interval, and it becomes smaller in the later observation interval. In all the cases, the proposed algorithm can accurately detect the amplitude variation.
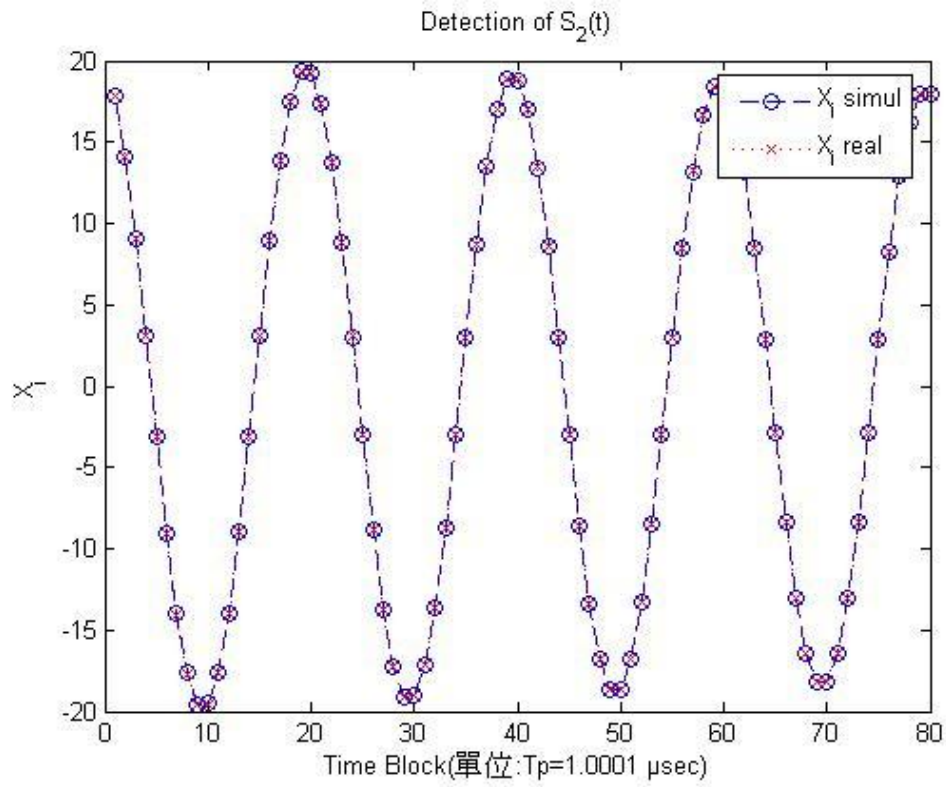
17

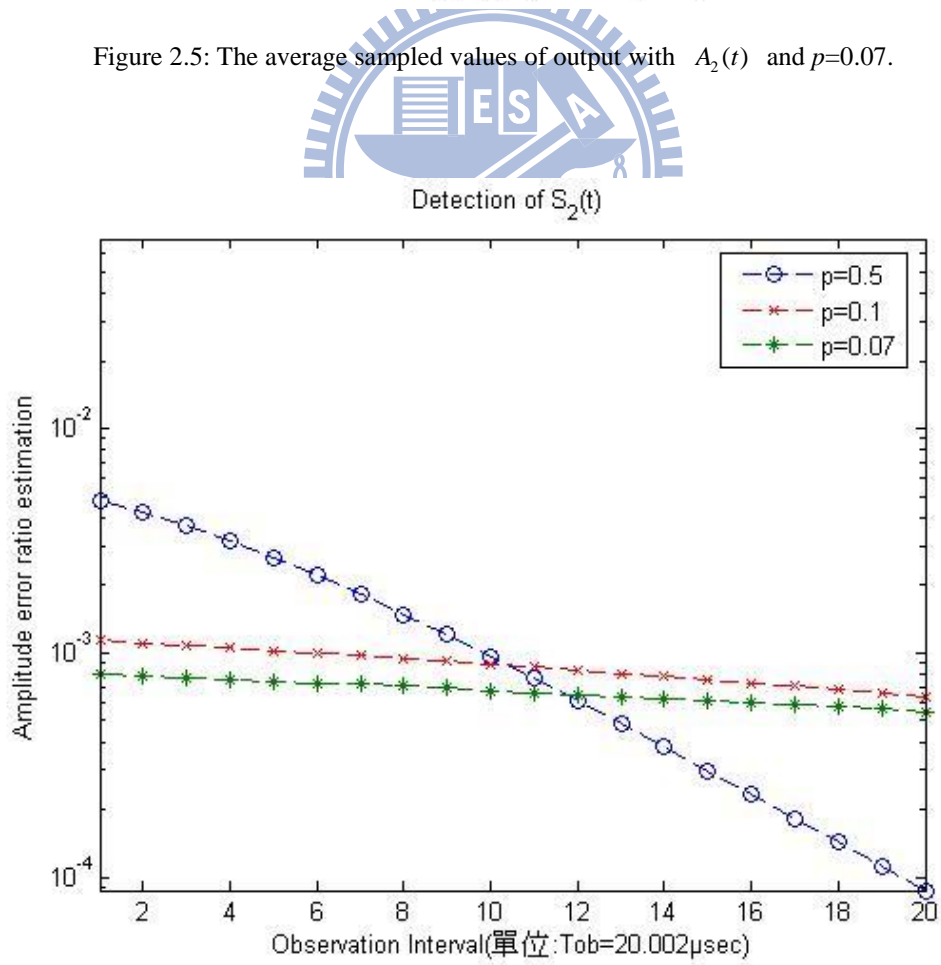Figure 2.5: The average sampled values of output with $A_2(t)$ and p=0.07.

Figure 2.6: Amplitude Error Ratio with $A_2(t)$ under different p.

Next we will run the simulation for different phase shifts. In practice the phase varies on transmitting through air, too. The variation of phase is random. We assume $\phi_{2,i}$ in the time interval $iT_{ob} \le t \le (i+1)T_{ob}$ as

$$\begin{cases} \phi_{2,i} = \phi_{2,i-1} + c_i \cdot \Delta\phi & , i = 1, 2, \ldots \\ \phi_{2,0} = \phi_2 \end{cases} \tag{2.53}$$

where $c_i : \pm 1$ is an random variable and $c_0 = 0$.

$\Delta\phi$: The phase shift of each time interval $iT_{ob} \le t \le (i+1)T_{ob}$.

Note that the phase during each time interval T_{ob} is assumed to be constant, but the phase shifts $\Delta\phi$ in the next time interval T_{ob}, see Figure 2.7 for the random phase variation. The average sampled values of output x_i is shown in Figure 2.8. We find that the algorithm can detect the signal $S_2(t)$ under the random variation of phase.

Figure 2.9 and Figure 2.10 show the simulation results under different $\Delta\phi$ where the Amplitude Error Ratio and Phase Shift Error Ratio are small under this case. We can find Phase Shift Error Ratio rises when $\Delta\phi$ is close to $180°$. It is because the phase varies too large to be detected precisely.
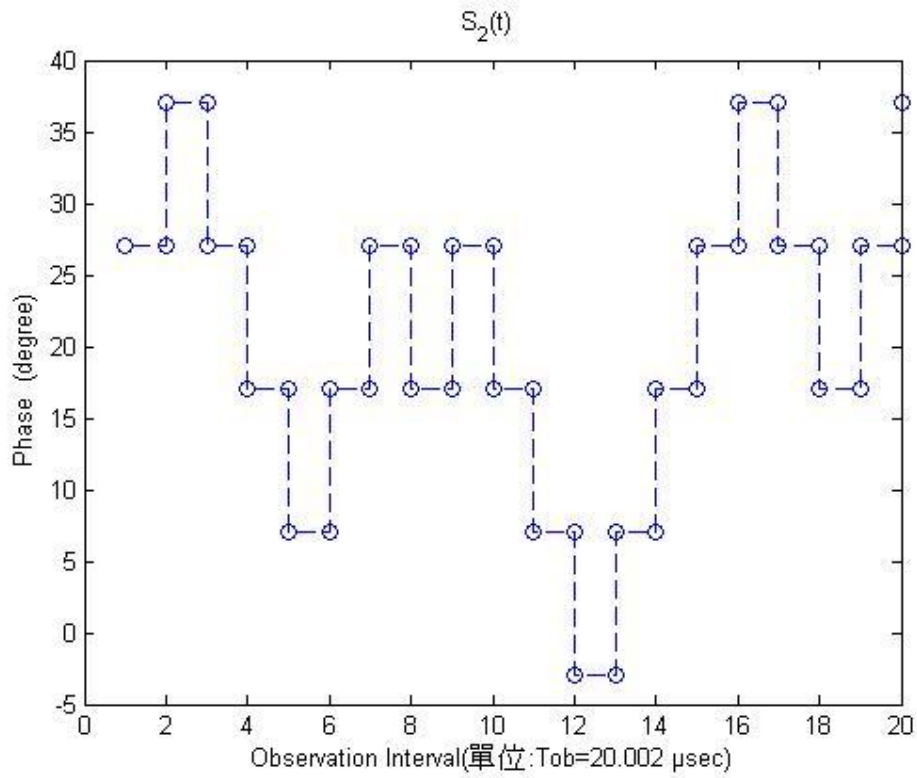
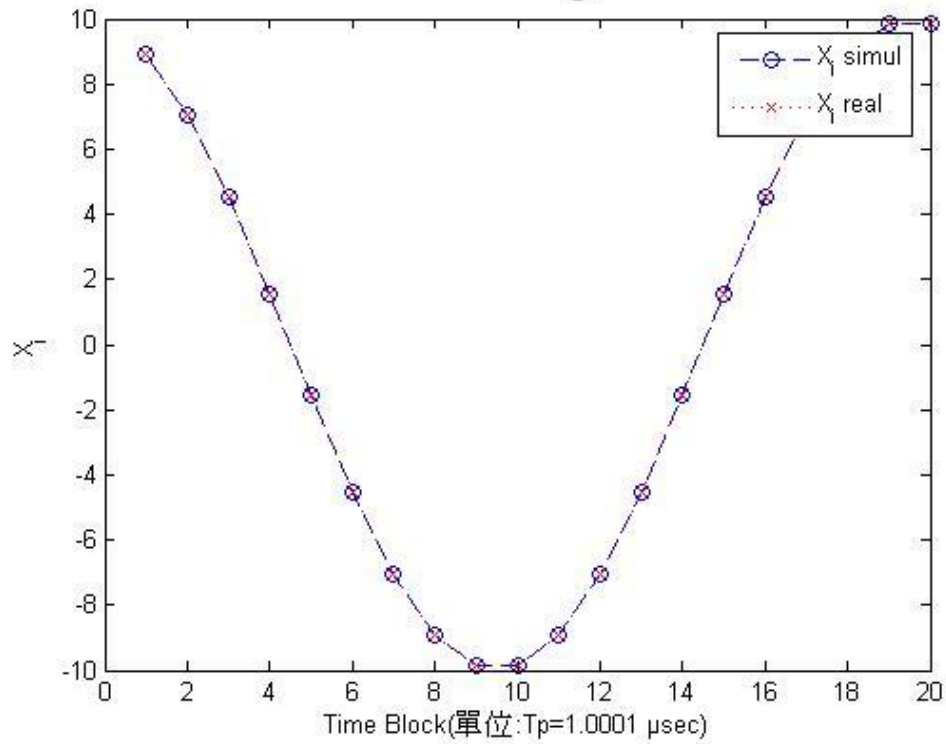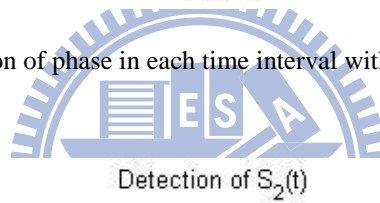Figure 2.7: The variation of phase in each time interval with $\Delta\phi = 10°$ and $\phi_2 = 27°$.

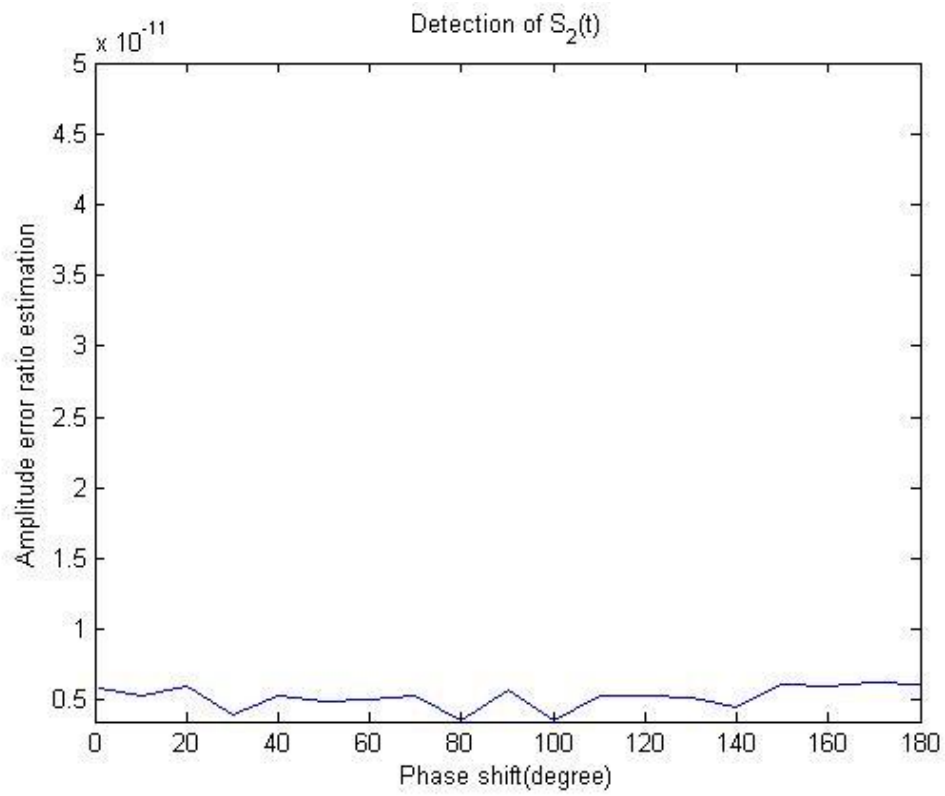Figure 2.8: The average sampled values of output x_i with $\Delta\phi = 10°$.

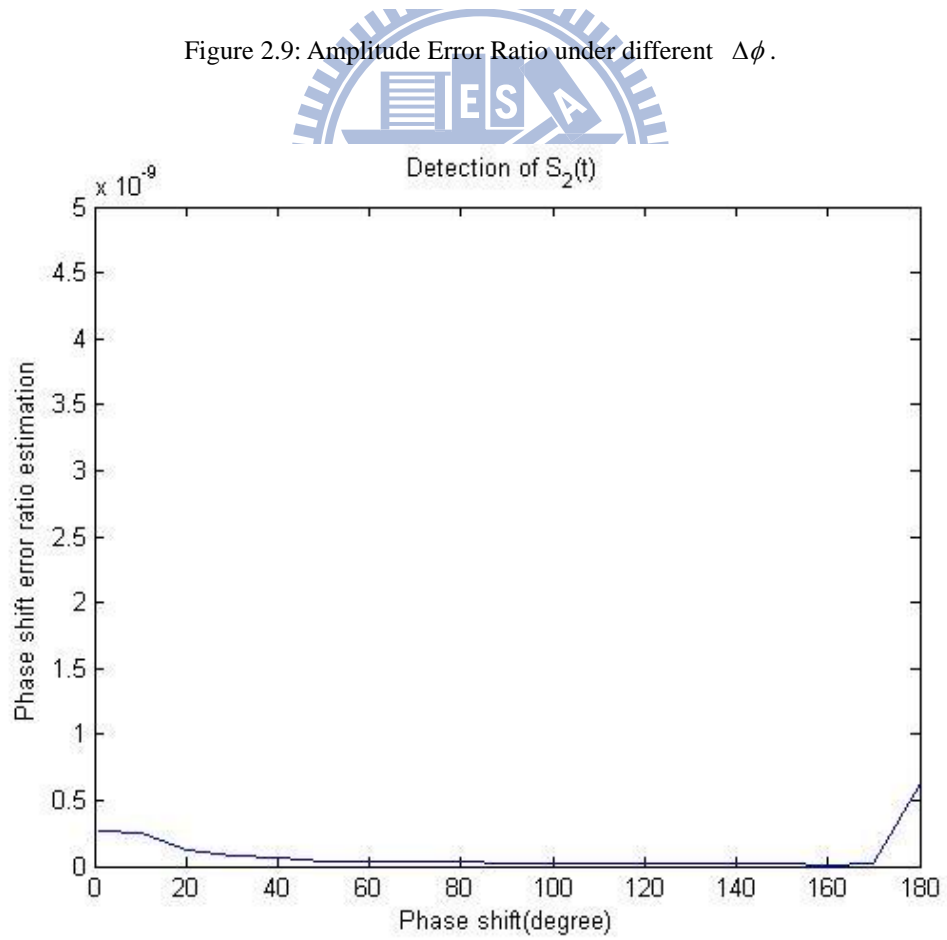Figure 2.9: Amplitude Error Ratio under different $\Delta\phi$.

Figure 2.10: Phase Shift Error Ratio under different $\Delta\phi$.

21

Next we will combine amplitude and phase variations to test our detection algorithm whether it can work in more complex situations. Thus $s_2(t)$ is written as

$$s_2(t) = A_2(1+e^{-p\frac{t}{T}}) \cdot \cos(w_2 t + \phi_2(t)) \tag{2.54}$$

where $\phi_{2,i} = \phi_2(iT_p)$ according to Eq. (2.53).

Figure 2.11 shows that the average sampled values of output x_i, which follows the amplitude variation of $s_2(t)$ accurately with time. The simulation results are shown in Figure 2.12 and Figure 2.13 where the Amplitude Error Ratio and Phase Shift Error Ratio are small under this case.
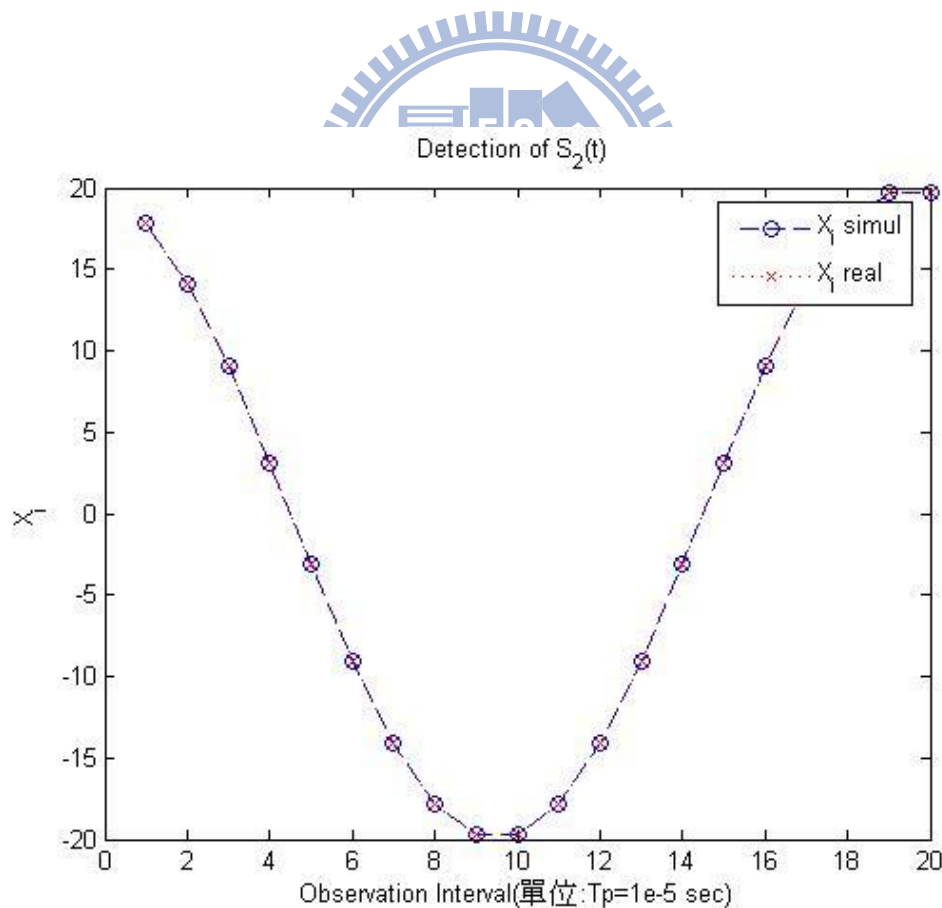

Figure 2.11: The average sampled values of output x_i with p=0.07, T=4x10^{-5} s, $\Delta\phi$ =10° and ϕ_2 =27°.

22

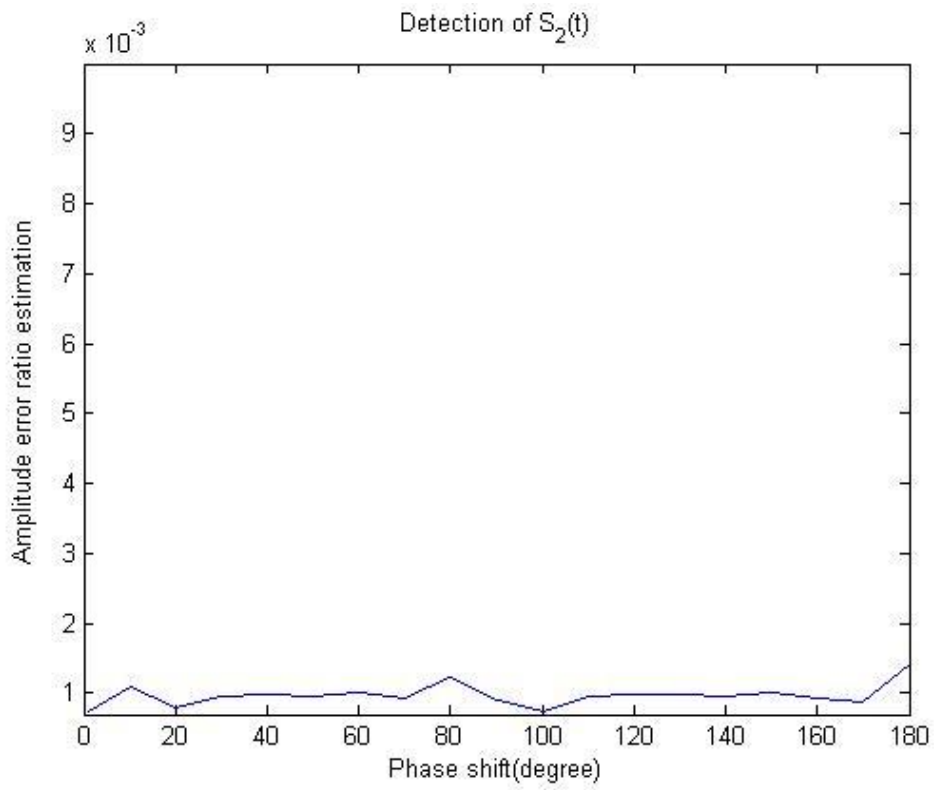Figure 2.12: Amplitude Error Ratio under different $\Delta\phi$.
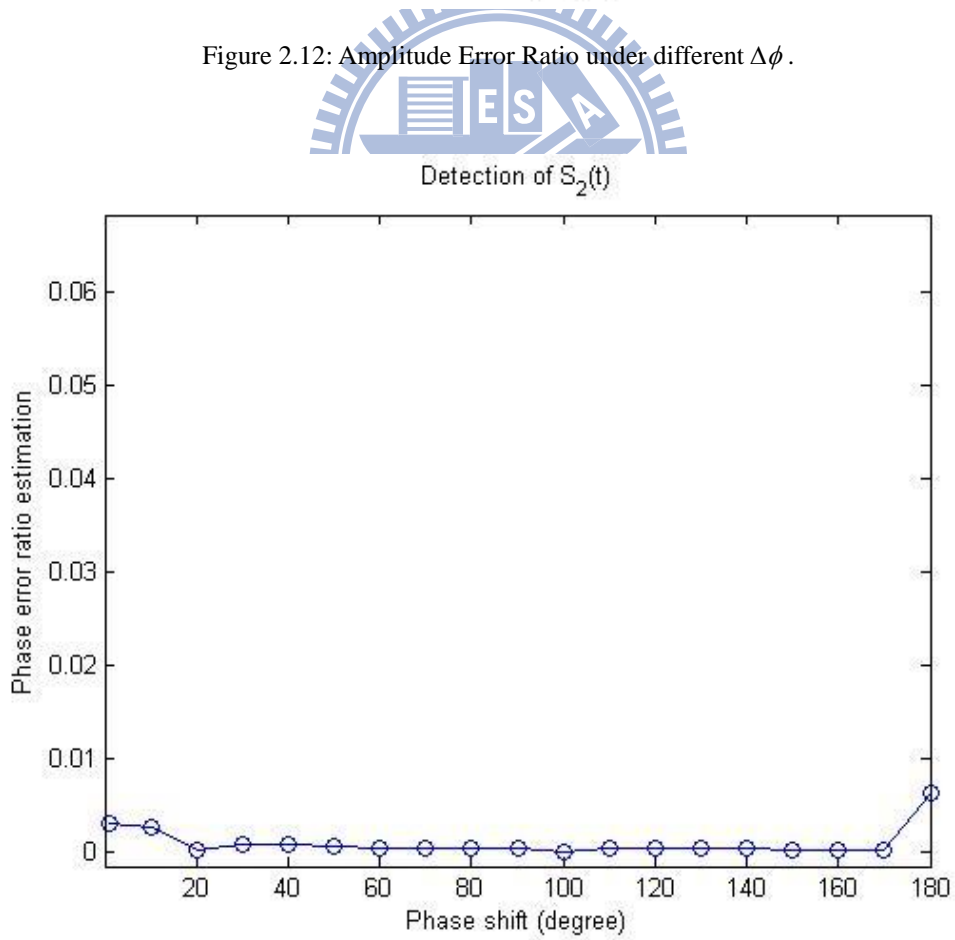
Detection of S$_2$(t)

Figure 2.13: Phase Shift Error Ratio under different $\Delta\phi$.

2.3.2 Simulation results with detection of $s_1(t)$

We will follow the same steps as the simulation of detecting $s_2(t)$ in this section. In the beginning, we set the parameters of simulation as the table below:

Tab. 2.2: System Parameters for the Simulation of Detection Algorithm for $s_1(t)$.	
Number of samples	W =122
(β, l, h)	(5 , 4, 121)
Phase of $s_1(t)$	ϕ_1 =33°
Phase of $s_2(t)$	ϕ_2 =27°
Frequency of $s_1(t)$	f_1 =610 *MHz*
Frequency of $s_2(t)$	f_2 =609 *MHz*
Sample interval	t_s' = 8.1967 *ns*
Time blocks	T_p' =1.0001 *μs*
Number of T_p'	M =20
Time delay	τ' = 0.081967 *ns*
Observation interval	T_{ob}' = 20.002 *μs*
Number of T_{ob}'	q =20

Note that the parameters setting above satisfy Eqs. (2.34) and (2.37). The simulation results under different A_1 / A_2 ratios are shown in Figure 2.14 and Figure 2.15 where the amplitude and phase are constants with time. We can find that Amplitude Error Ratio is very small between $10^{-9} \sim 10^{-11}$, which

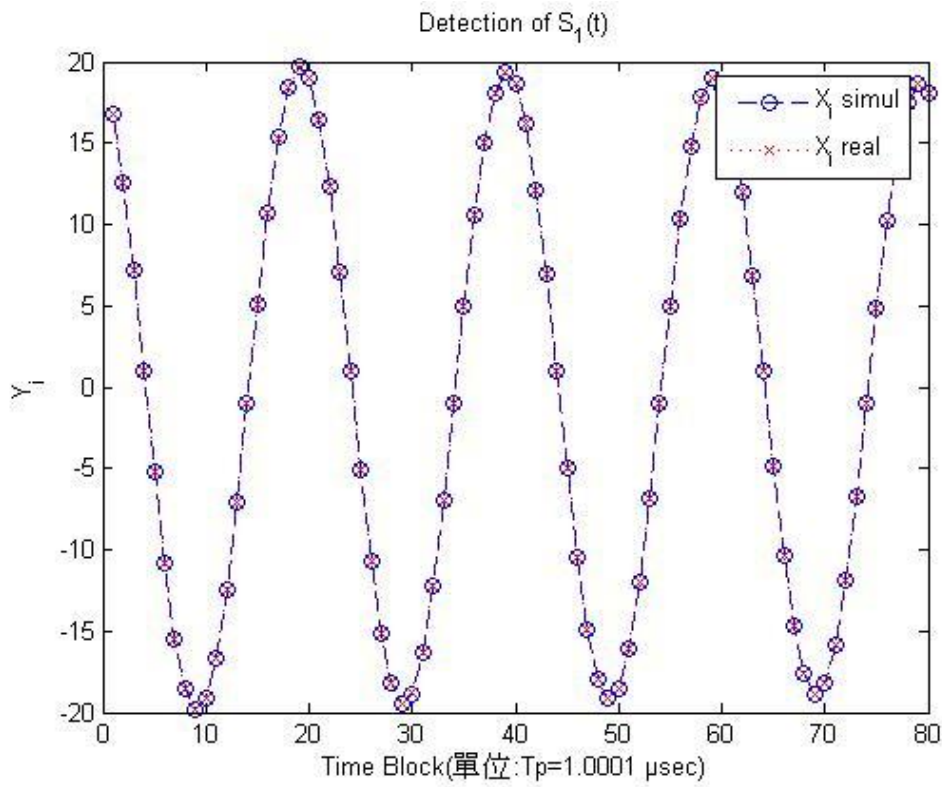means the amplitude of $s_1(t)$ can be accurately detected.

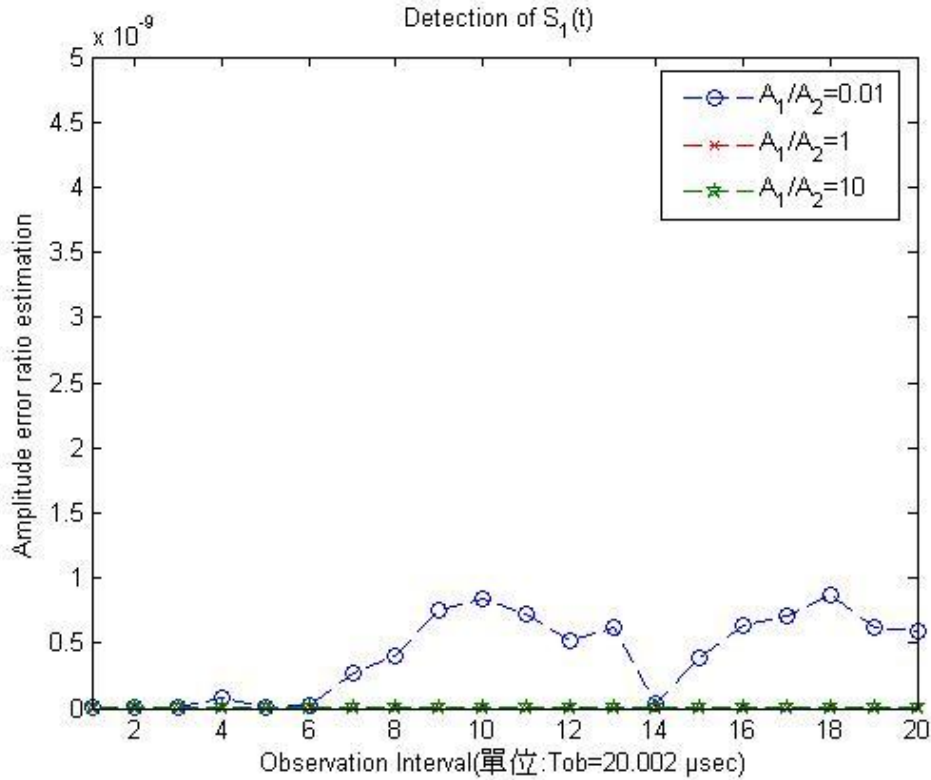Figure 2.14: The average sampled values of output y_i when $A_1 = A_2 = 1$.

Figure 2.15: Amplitude Error Ratio under different A_1 / A_2.

25

In the second case, we assume $A_1(t)$ varies with time as $A_1(t) = A_1 \cdot (1 + e^{-p\frac{t}{T}})$ and $A_1 = A_2 = 10$, p=0.07 or 0.1 or 0.5, and T=4x10^{-5} s. Figure 2.16 shows Amplitude Error Ratio with different p. The amplitude varies faster when p is large. Thus the Amplitude Error Ratio increases in the earlier observation interval, and it becomes smaller in the later observation interval. Apparently, the proposed algorithm still can accurately detect the variation.
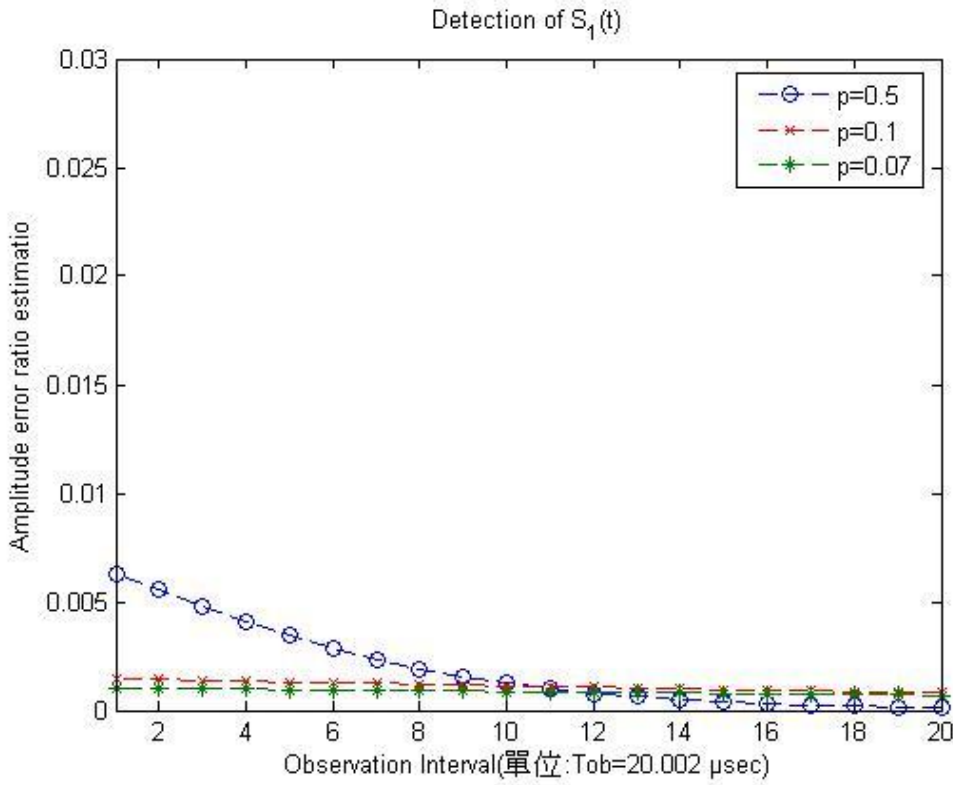
Figure 2.16: Amplitude Error Ratio with $A_1(t)$ under different p.

Next, we assume $\phi_{1,i} = \phi_{1,i-1} + c_i \square \Delta\phi, i = 1,2,...q$, and $\phi_{1,0} = \phi_1$ in the time interval $iT_{ob}' \leq t \leq (i+1)T_{ob}'$, where $c_i = \pm 1$ is a random variable and $c_0 = 0$, $\Delta\phi$ is the phase shift of each time interval $iT_{ob}' \leq t \leq (i+1)T_{ob}'$. Note that the phase during each time interval T_{ob}' is constant, but the phase varies $\Delta\phi$ in the next time interval. Figure 2.17 and Figure 2.18 show the simulation results under different

$\Delta\phi$.

Figure 2.17: Amplitude Error Ratio under different $\Delta\phi$.
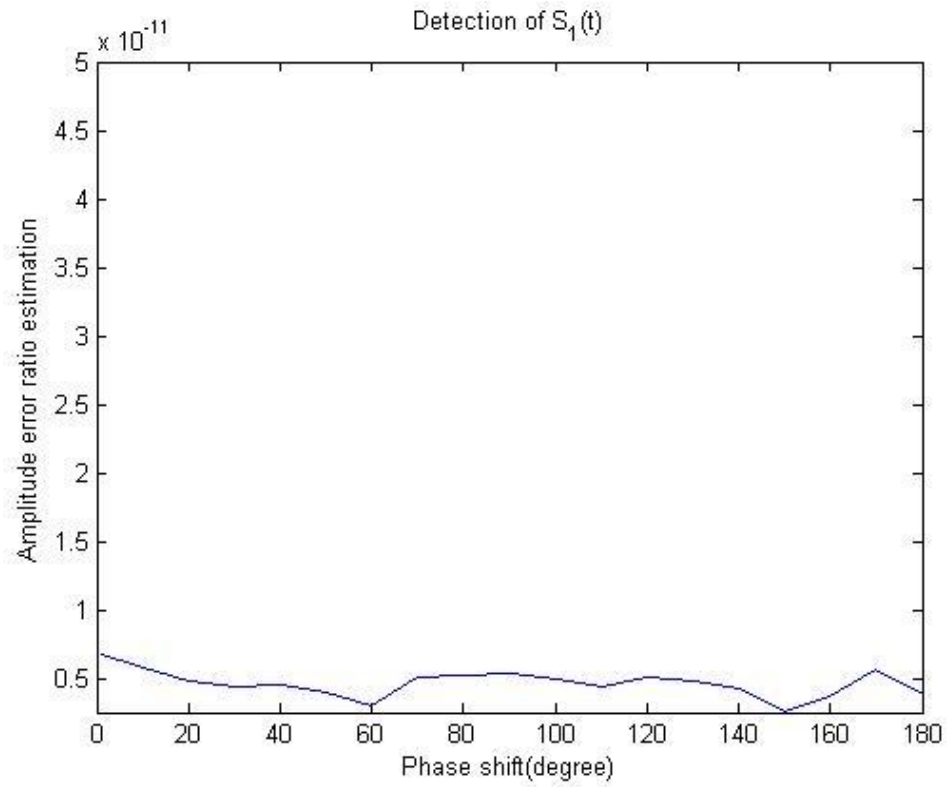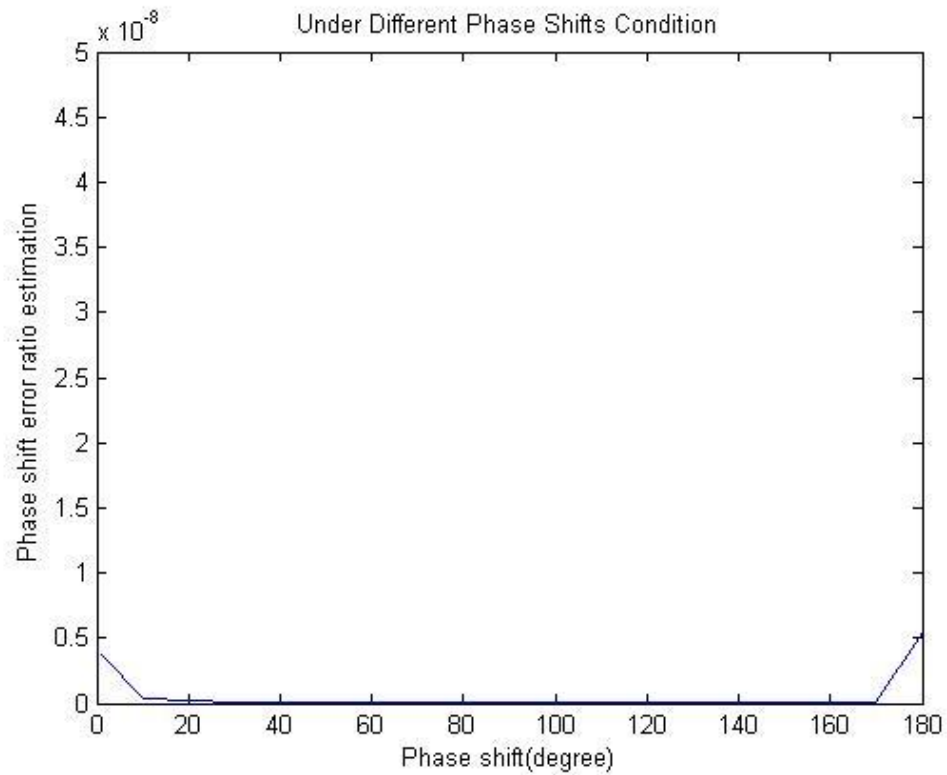

Figure 2.18: Phase Shift Error Ratio under different $\Delta\phi$.

27

Further, we combine all the cases above to test our detection algorithm in more complex situations. Here $S_1(t)$ is written as $s_1(t) = A_1(1 + e^{-p\frac{t}{T}}) \cdot \cos(w_1 t + \phi_1(t))$, where $\phi_{1,i} = \phi_1(iT_p)$ according to Eq. (2.53). The simulation results are shown in Figure 2.19 and Figure 2.20. The Amplitude Error Ratio and Phase Shift Error Ratio are acceptable under this case. Consequently, our algorithm can detect the amplitude and the phase variations of $s_1(t)$ and $s_2(t)$ under noiseless environment.

Figure 2.19: Amplitude Error Ratio under different $\Delta\phi$.
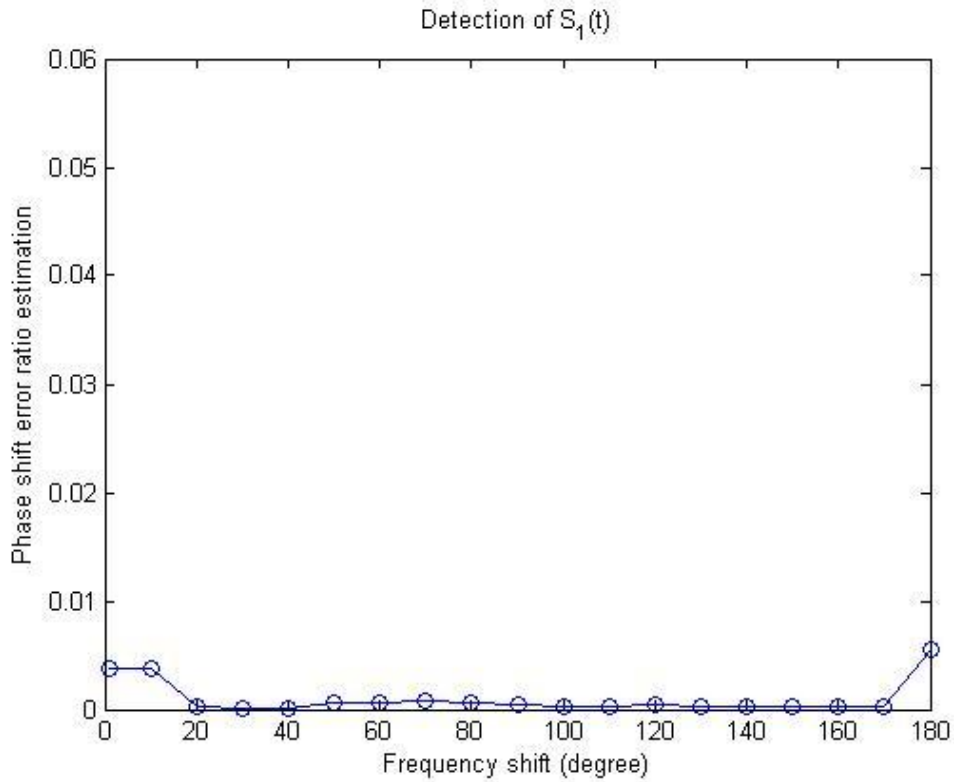
Figure 2.20: Phase Shift Error Ratio under different $\Delta\phi$.
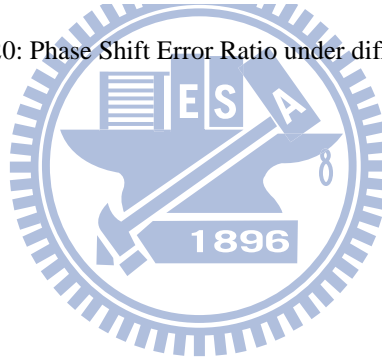
2.4 Summary
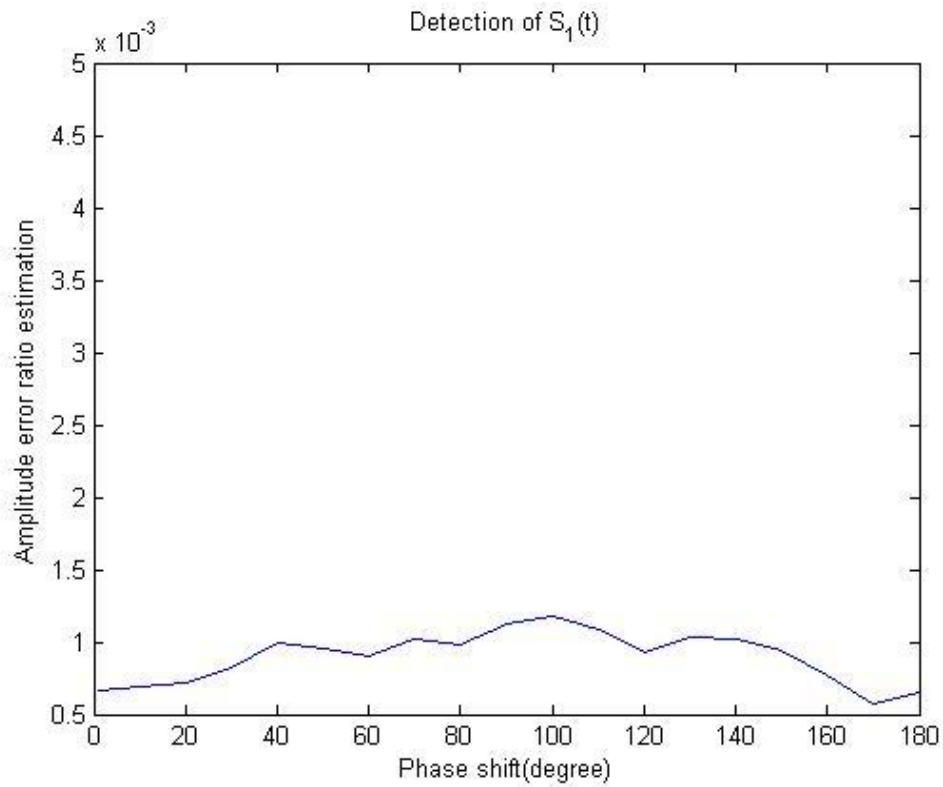
The proposed algorithm has two steps for the detection of the received signal. First s, we estimate the amplitude of $s_1(t)$ or $s_2(t)$ from the sample values using Eq. (2.24). Second, we estimate the phase variations of $s_1(t)$ or $s_2(t)$ between the time interval $iT_{ob} \le t \le (i+1)T_{ob}$. It is important to estimate the amplitude accurately in the first step, which will affect the accuracy of phase estimation. From the simulation results above, we find the algorithm is more sensitive to the amplitude variation than the phase variation. When the amplitude varies with time, the estimation error may increase from 10^{-9} to 10^{-3}, especially for the phase shift error.

Chapter 3

Performance Analysis

In the chapter, we discuss the performance due to frequency offset and noise. We will derive frequency offset effect and noise effect of our algorithm in detail, and present some simulation results to verify the error performance of the system.

3.1 Frequency Offset Effect

3.1.1 When $s_1(t)$ has frequency offset $\Delta \omega_1$

In the receiver, the signal frequency might vary with time. It will affect the accuracy of the detection. In this section we intend to analyze the influence arising from frequency offset on detecting $s_2(t)$. When there is frequency offset in $s_1(t)$, the received signal $r(t)$ will be

$$r(t) = A_1 \cos[(w_1 + \Delta \omega_1)t + \phi_1] + A_2 \cos(w_2 t + \phi_2) \tag{3.1}$$

Assume $r(t)$ is sampled at $t = kt_s$, $k = 0,1,2,...N-1$ and $t_s = (m + \dfrac{1}{N})T_1 = \alpha T_2$, we obtain

$$r(k) = r(kt_s) = s_1(k) + s_2(k)$$

where

$$
\begin{aligned}
s_1(k) &= A_1 \cos[(w_1 + \Delta \omega_1)kt_s + \phi_1] \\
&= A_1 \cos(w_1 kt_s + \Delta \omega_1 kt_s + \phi_1) = A_1 \cos(2\pi \frac{k}{N} + \Delta \omega_1 kt_s + \phi_1)
\end{aligned} \tag{3.2}
$$

Consider

$$\sum_{k=0}^{N-1} s_1(k) = \sum_{k=0}^{N/2-1} [s_1(k) + s_1(k+N/2)]$$

$$= A_1 \sum_{k=0}^{N/2-1} \{\cos(2\pi \frac{k}{N} + \Delta\omega_1 k t_s + \phi_1) + \cos[2\pi \frac{k+N/2}{N} + \Delta\omega_1(k+N/2)t_s + \phi_1]\}$$

$$= 2A_1 \sum_{k=0}^{N/2-1} \{\cos[2\pi \frac{k}{N} + \pi/2 + \Delta\omega_1(k+N/4)t_s + \phi_1]\cos(\pi/2 + \Delta\omega_1 \frac{N}{4}t_s)\}$$

$$= 2A_1 \sin(\Delta\omega_1 \frac{N}{4}t_s) \sum_{k=0}^{N/2-1} \sin[2\pi \frac{k}{N} + \Delta\omega_1(k+N/4)t_s + \phi_1] \qquad (3.3)$$

Thus we can rewrite Eq. (2.14)

$$x_0 = \frac{1}{N}\sum_{k=0}^{N-1} r(k) = \frac{1}{N}\sum_{k=0}^{N-1} [s_1(k) + s_2(k)]$$

$$= \frac{2A_1}{N}\sin(\Delta\omega_1 \frac{N}{4}t_s) \sum_{k=0}^{N/2-1} \sin[2\pi \frac{k}{N} + \Delta\omega_1(k+N/4)t_s + \phi_1] + A_2\cos\phi_2 \qquad (3.4)$$

Next consider the time interval $T_p \le t \le 2T_p$ and $T_p = Nt_s + \tau$. Again we take N samples at

$t = T_p + jt_s$, $j=0,1,2,...,N-1$, and have zero samples within $T_p + Nt_s \le t \le 2T_p$. In this case Eq. (2.15) is

written as

$$r(j) = r(T_p + jt_s)$$

$$= A_1\cos[(w_1 + \Delta\omega_1)(T_p + jt_s) + \phi_1] + A_2\cos[w_2(T_p + jt_s) + \phi_2]$$

$$= A_1\cos[w_1(Nt_s + jt_s + \tau) + \Delta\omega_1(Nt_s + jt_s + \tau) + \phi_1] + A_2\cos[w_2(Nt_s + jt_s + \tau) + \phi_2]$$

$$= A_1\cos[2\pi \frac{j}{N} + (w_1 + \Delta\omega_1)\tau + \Delta\omega_1(N+j)t_s + \phi_1] + A_2\cos[w_2(Nt_s + jt_s + \tau) + \phi_2] \qquad (3.5)$$

where

$$\sum_{j=0}^{N-1} A_1 \cos[2\pi \frac{j}{N} + (w_1 + \Delta\omega_1)\tau + \Delta\omega_1(N+j)t_s + \phi_1]$$

$$= A_1 \square \sum_{j=0}^{N/2-1} \{\cos[2\pi \frac{j}{N} + (w_1 + \Delta\omega_1)\tau + \Delta\omega_1(N+j)t_s + \phi_1]$$

$$+ \cos[2\pi \frac{j}{N} + \pi/2 + (w_1 + \Delta\omega_1)\tau + \Delta\omega_1(N+j+N/2)t_s + \phi_1]\}$$

$$= 2A_1 \square \sum_{j=0}^{N/2-1} \{\cos[2\pi \frac{j}{N} + \pi/2 + (w_1 + \Delta\omega_1)\tau + \Delta\omega_1(N+j+N/4)t_s + \phi_1]$$

$$\square \cos(\pi/2 + \Delta\omega_1 \frac{N}{4}t_s)\}$$

$$= 2A_1 \sin(\Delta\omega_1 \frac{N}{4}t_s) \square \sum_{j=0}^{N/2-1} \sin[2\pi \frac{j}{N} + (w_1 + \Delta\omega_1)\tau + \Delta\omega_1(N+j+N/4)t_s + \phi_1] \qquad (3.6)$$

Thus we can rewrite Eq. (2.18) as

$$x_1 = \frac{1}{N}\sum_{j=0}^{N-1} r(j) = 2\frac{A_1}{N}\sin(\Delta\omega_1 \frac{N}{4}t_s) \square \sum_{j=0}^{N/2-1} \sin[2\pi \frac{j}{N} + (w_1 + \Delta\omega_1)\tau + \Delta\omega_1(N+j+N/4)t_s + \phi_1]$$
$$+ A_2 \cos(w_2\tau + \phi_2) \qquad (3.7)$$

In general, we will obtain the average for the time block $iT_p \le t \le (i+1)T_p$ as

$$x_i' = A_2 \cos[w_2(i\tau) + \phi_2] +$$
$$2\frac{A_1}{N}\sin(\Delta\omega_1 \frac{N}{4}t_s) \square \sum_{j=0}^{N/2-1} \sin[2\pi \frac{j}{N} + (w_1 + \Delta\omega_1)i\tau + \Delta\omega_1(iN+j+N/4)t_s + \phi_1]$$
$$= x_i + \Delta x_i \qquad (3.8)$$

where

$$\Delta x_i = 2\frac{A_1}{N}\sin(\Delta\omega_1 \frac{N}{4}t_s) \square \sum_{j=0}^{N/2-1} \sin[2\pi \frac{j}{N} + (w_1 + \Delta\omega_1)i\tau + \Delta\omega_1(iN+j+N/4)t_s + \phi_1] \qquad (3.9)$$

and the time delay τ is still chosen as $\tau = T_2 / M$.

From Eq. (2.24) we can estimate A_2 as

$$
\begin{aligned}
\hat{A}'_2 &= \sqrt{\frac{2}{M} \cdot \sum_{i=0}^{M-1} x_i'^2} = \sqrt{\frac{2}{M} \cdot \sum_{i=0}^{M-1} (x_i + \Delta x_i)^2} \\
&= \sqrt{\frac{2}{M} \cdot \sum_{i=0}^{M-1} (x_i^2 + 2x_i \square \Delta x_i + \Delta x_i^2)} \\
&= \sqrt{\frac{2}{M} \cdot \sum_{i=0}^{M-1} x_i^2 \cdot + \frac{2}{M} \sum_{i=0}^{M-1} (2x_i \square \Delta x_i + \Delta x_i^2)} \\
&= \sqrt{\hat{A}_2 \cdot + \Delta A}
\end{aligned}
\tag{3.10}
$$

where

$$
\Delta A = \frac{2}{M} \sum_{i=0}^{M-1} (2x_i \square \Delta x_i + \Delta x_i^2)
\tag{3.11}
$$

Then we can estimate $A'_{2,k}$ with the method just derived. As a consequence, we will obtain a set of estimated amplitudes $(A'_{2,0}, A'_{2,1}, ..., A'_{2,q-1})$. Then we can estimate phase shift using Eq. (2.27) as

$$
\begin{aligned}
\Delta\phi'_{k,k+1} &= \cos^{-1}\left\{ \frac{1}{A'_{2,k} \cdot A'_{2,k+1}} [\frac{A'^2_{2,k} + A'^2_{2,k+1}}{2} - \frac{1}{M} \sum_{i=0}^{M-1} (x'_{k,i} - x'_{k+1,i})^2] \right\} \\
&= \cos^{-1}\left\{ \frac{1}{A'_{2,k} \cdot A'_{2,k+1}} [\frac{A'^2_{2,k} + A'^2_{2,k+1}}{2} - \frac{1}{M} \sum_{i=0}^{M-1} (x_{k,i} - x_{k+1,i} + \Delta x_{k,i} - \Delta x_{k+1,i})^2] \right\} \\
&\approx \cos^{-1}\left\{ \frac{1}{A'_{2,k} \cdot A'_{2,k+1}} [\frac{A'^2_{2,k} + A'^2_{2,k+1}}{2} - \frac{1}{M} \sum_{i=0}^{M-1} (x_{k,i} - x_{k+1,i})^2] \right\}
\end{aligned}
\tag{3.12}
$$

Usually, the frequency offset is small between $kT_{ob} \leq t \leq (k+1)T_{ob}$, thus we can let $\Delta x_{k,i} - \Delta x_{k+1,i} \approx 0$ where $A'_{2\,k+1} = A_{2\,k+1} + \Delta A_{k+1}$, and $A'_{2,k} = A_{2,k} + \Delta A_{2,k}$.

33

3.1.2 When $s_2(t)$ has frequency offset $\Delta\omega_2$

Next, we consider $s_2(t)$ with the frequency offset $\Delta\omega_2$. Then the received signal $r(t)$ will be

$$r(t) = A_1\cos(w_1 t + \phi_1) + A_2\cos[(w_2 + \Delta\omega_2)t + \phi_2] = s_1(t) + s_2(t) \tag{3.13}$$

Assume $r(t)$ is sampled at $t = kt_s$, $k = 0,1,2,...N-1$ and $t_s = (m + \dfrac{1}{N})T_1 = \alpha T_2$, then

$$r(k) = r(kt_s) = s_1(k) + s_2(k)$$

where

$$s_2(k) = s_2(kt_s) = A_2\cos[(w_2 + \Delta\omega_2)kt_s + \phi_2]$$
$$= A_2\cos(w_2 kt_s + \Delta\omega_2 kt_s + \phi_2) = A_2\cos(\Delta\omega_2 kt_s + \phi_2) \tag{3.14}$$

Thus we can rewrite Eq. (2.14) as

$$x_0 = \frac{1}{N}\sum_{k=0}^{N-1} r(k) = \frac{1}{N}\sum_{k=0}^{N-1}[s_1(k) + s_2(k)]$$
$$= \frac{A_2}{N}\sum_{k=0}^{N-1}\cos(\Delta\omega_2 kt_s + \phi_2) \tag{3.15}$$

Now consider the time interval $T_p \le t \le 2T_p$ and $T_p = Nt_s + \tau$. Again we take N samples at

$t = T_p + jt_s$, $j=0,1,2,...,N-1$, and have zero samples within $T_p + Nt_s \le t \le 2T_p$. In this case Eq. (2.14)

becomes

$$r(j) = r(T_p + jt_s)$$
$$= A_1\cos[w_1(T_p + jt_s) + \phi_1] + A_2\cos[(w_2 + \Delta\omega_2)(T_p + jt_s) + \phi_2]$$
$$= A_1\cos(2\pi\frac{j}{N} + w_1\tau + \phi_1) + A_2\cos[(w_2 + \Delta\omega_2)(Nt_s + jt_s + \tau) + \phi_2]$$
$$= A_1\cos(2\pi\frac{j}{N} + w_1\tau + \phi_1) + A_2\cos[w_2\tau + \Delta\omega_2((N+j)t_s + \tau) + \phi_2]$$
$$\tag{3.16}$$

Hence

$$x_1 = \frac{1}{N} \sum_{j=0}^{N-1} r(j)$$

$$= \frac{A_2}{N} \square \sum_{j=0}^{N-1} \cos[w_2 \tau + \Delta \omega_2 ((N+j)t_s + \tau) + \phi_2] \qquad (3.17)$$

In general, we will obtain the average for the time block $iT_p \le t \le (i+1)T_p$ as

$$x_i' = \frac{A_2}{N} \square \sum_{j=0}^{N-1} \cos[w_2(i\tau) + \Delta \omega_2((iN+j)t_s + i\tau) + \phi_2] \qquad (3.18)$$

and

$$A_2 \square \sum_{j=0}^{N-1} \cos[w_2 i\tau + \Delta \omega_2((iN+j)t_s + \tau) + \phi_2]$$

$$= A_2 \square \sum_{j=0}^{N-1} \cos[(w_2 i\tau + \phi_2) + \Delta \omega_2((iN+j)t_s + \tau)]$$

$$= A_2 \square \sum_{j=0}^{N-1} \{\cos(w_2 i\tau + \phi_2)\cos[\Delta \omega_2((iN+j)t_s + i\tau)] - \sin(w_2 i\tau + \phi_2)\sin[\Delta \omega_2((iN+j)t_s + i\tau)]\} \qquad (3.19)$$

Further Eq. (3.18) can be written as

$$x_i' = x_i \square \frac{1}{N} \sum_{j=0}^{N-1} \cos[\Delta \omega_2((iN+j)t_s + i\tau)] - \frac{A_2}{N} \sin(w_2 i\tau + \phi_2) \square \sum_{j=0}^{N-1} \sin[\Delta \omega_2((iN+j)t_s + i\tau)] \qquad (3.20)$$

and the time delay τ is also chosen as $\tau = T_2 / M$.

Thus, using Eq. (2.23) we can estimate A_2 between each time interval T_p . Further, we can estimate phase shift $\Delta \phi_{k,k+1}$ for the time block $kT_p \le t \le (k+1)T_p$ using Eq. (2.27).

3.1.3 Simulation results with frequency offset

After analyzing the algorithm with frequency offset mathematically, we perform the simulation in the following. First we consider the detection of $s_2(t)$ when $s_1(t)$ has frequency offset $\Delta\omega_1$.

A. Frequency offset $\Delta\omega_1$

Figure 3.1 shows the Amplitude Error Ratio versus $\Delta f_1 / f_1$ when $f_1 = 610$ MHz and phase shift $\Delta\phi = 20°$. The normalized frequency offset $\Delta f_1 / f_1$ ranges from $10^{-6} \sim 10^{-4}$, and the Amplitude Error Ratio is around 10^{-3}. The Phase Error Ratio under different $\Delta f_1 / f_1$ is shown in Figure 3.2, where the error ratio is under $10^{-3} \sim 10^{-1}$ and the maximum phase shift error reaches $0.96°$ when $\Delta f_1 / f_1 = 4\text{x}10^{-5}$ ($\therefore \Delta f_2 = 2440$ Hz). The simulation results are acceptable in the case.
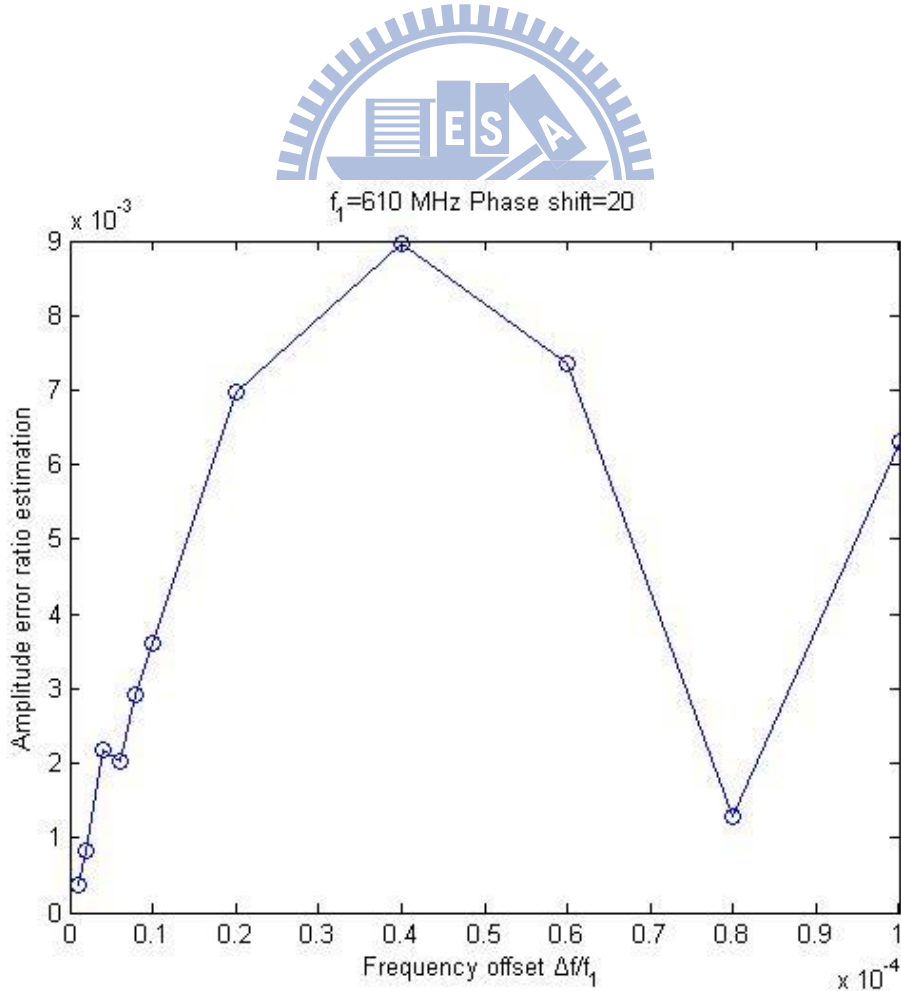

Figure 3.1: Amplitude Error Ratio under different $\Delta f_1 / f_1$.
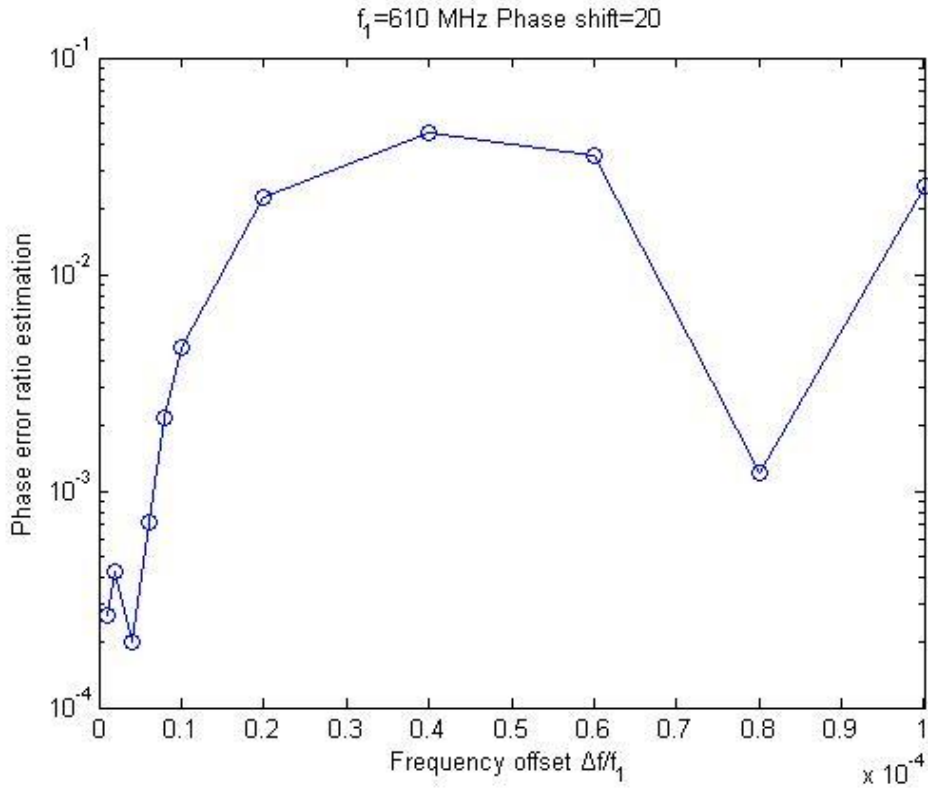
Figure 3.2: Phase Shift Error Ratio under different $\Delta f_1 / f_1$.

B. Frequency offset $\Delta\omega_2$

Next, we carry out the simulation of detecting $s_2(t)$ when $s_2(t)$ has frequency offset $\Delta\omega_2$. Figure 3.3 and Figure 3.4 show the Amplitude Error Ratio and Phase Shift Error Ratio with respect to $\Delta f_2 / f_2$ when f_2=609 MHz and phase shift $\Delta\phi$=20° where the normalized frequency offset $\Delta f_2 / f_2$ ranges between $10^{-6} \sim 10^{-4}$. We find the Phase Shift Error Ratio rises obviously, and the phase shift error is above 4°, even over 40°,when $\Delta f_2 / f_2 > 1\text{x}10^{-6}$ (∴ Δf_2>609 Hz). Our algorithm can't work well in the condition, thus the simulation results present that the influence on estimating phase shift is large when $s_2(t)$ has frequency offset $\Delta\omega_2$.
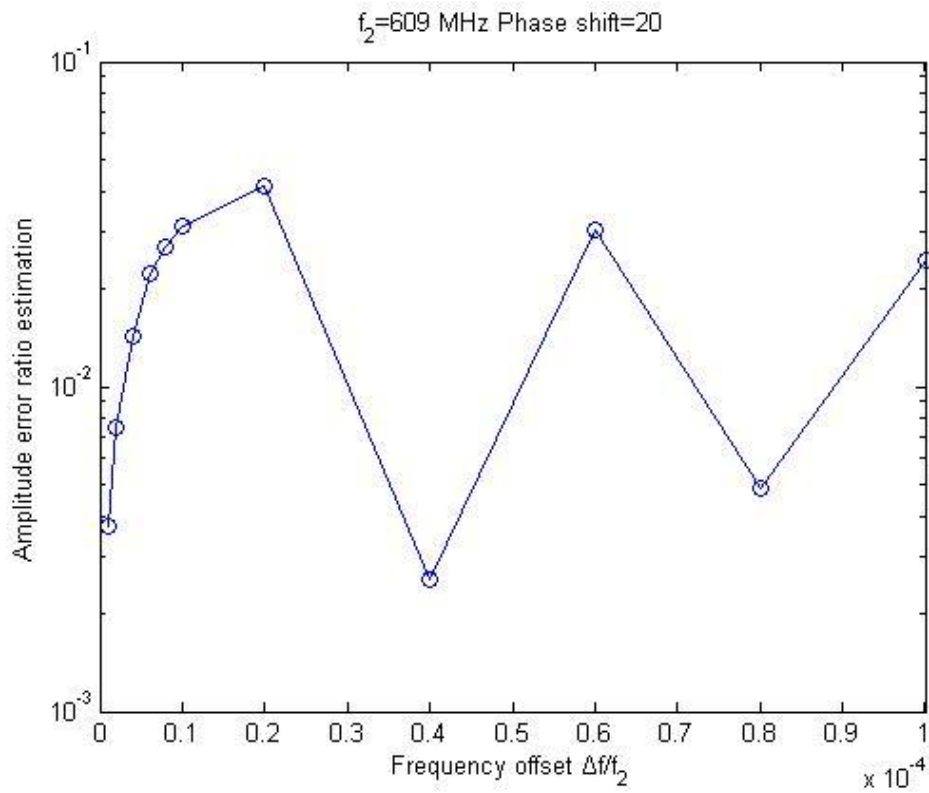
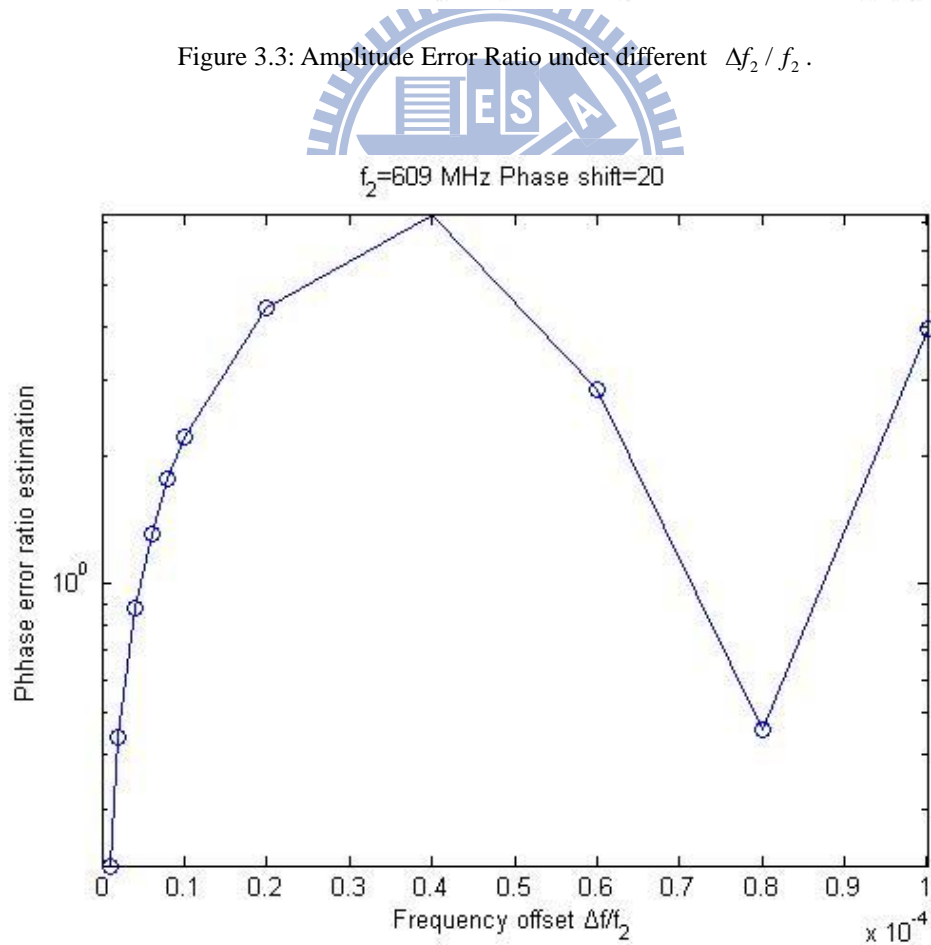Figure 3.3: Amplitude Error Ratio under different $\Delta f_2 / f_2$.

Figure 3.4: Phase Shift Error Ratio under different $\Delta f_2 / f_2$.

3.2 Noise Analysis

Any communication systems would be affected by noise in reality. In this section, we analyze the performance of our algorithm in noisy environment. Our discussion is based on the simulation outcomes of different **signal-to-noise ratio** (SNR) in dB. We implement Additive white Gaussian noise (AWGN) to simulate the different SNR in our system.

3.2.1 Noise effect

Previously, we assume $n(t) = 0$ for simplicity. In practice, noise exists in any communication system. We assume the channel is an AWGN channel and the noise $n(t) \sim N(0,\sigma)$ is a zero mean Gaussian noise with variance σ^2. The received signal $r(t)$ is

$$r(t) = s_1(t) + s_2(t) + n(t)$$
$$= A_1 \cos(w_1 t + \phi_1) + A_2 \cos(w_2 t + \phi_2) + n(t) \tag{3.21}$$

Using Eq. (2.7) and (2.9), we have

$$x_0 = \frac{1}{N} \sum_{k=0}^{N-1} r(k) = \frac{1}{N} \sum_{k=0}^{N-1} [s_1(k) + s_2(k) + n(k)]$$
$$= A_2 \cos\phi_2 + \frac{1}{N} \sum_{k=0}^{N-1} n_k \tag{3.22}$$

where $n_k = n(kt_s)$ k=0,1,2,…,N-1.

Next consider the time interval $T_p \leq t \leq 2T_p$. Again we take N samples at $t = T_p + jt_s$, $j=0,1,2,...,N-1$, and have zero samples within $T_p + Nt_s \leq t \leq 2T_p$. Therefore

$$r(j) = r(T_p + jt_s)$$
$$= A_1 \cos[w_1(T_p + jt_s) + \phi_1] + A_2 \cos[w_2(T_p + jt_s) + \phi_2] + n(T_p + jt_s)$$
$$= A_1 \cos(\frac{2\pi}{N} j + w_1\tau + \phi_1) + A_2 \cos(w_2\tau + \phi_2) + n(T_p + jt_s)$$

Thus

$$x_1 = \frac{1}{N} \sum_{j=0}^{N-1} r(j) = A_2 \cos(w_2\tau + \phi_2) + \frac{1}{N} \sum_{j=0}^{N-1} n(T_p + jt_s)$$

(3.24)

In general, we will obtain the average for the time block $iT_p \le t \le (i+1)T_p$ as

$$x'_i = A_2 \cos(w_2(i\tau) + \phi_2) + \frac{1}{N} \sum_{j=0}^{N-1} n_{ij}$$

$$= x_i + \Delta x_i$$

(3.25)

where

$$n_{ij} = n(iT_p + jt_s), \qquad j = 0, 1..$$

(3.26)

and

$$\Delta x_i = \frac{1}{N} \sum_{j=0}^{N-1} n_{ij}, \qquad i=0,1,2....M-1.$$

(3.27)

Then we can use equation Eqs. (2.48) and (2.49) to estimate $(A'_{2,0}, A'_{2,1},..., A'_{2,q-1})$ and $\Delta\phi'_{k,k+1}$.

3.2.2 SNR analysis

Here we will analyze **SNR (Signal-to-noise ratio)** of the proposed system. Since $n(t)$ is a Gaussian noise and it's samples n_{ij} is also Gaussian noise. Consider x'_i, the output of the system from Eq. (3.24) which is also Gaussian distributed. Then we can calculate the mean μ and variance σ_e^2. And the signal power is $P_{signal} = A_2^2 / 2$.

Consider

$$\mu = E[x'_i] = E[A_2 \cos(w_2 i\tau + \phi_2) + \frac{1}{N}\sum_{j=0}^{N-1} n_{ij}]$$

$$= A_2 \cos(w_2 i\tau + \phi_2) + \frac{1}{N}\sum_{j=0}^{N-1} E[n_{ij}]$$

$$= A_2 \cos(w_2 i\tau + \phi_2) \tag{3.28}$$

Because each n_{ij} is an AWGN, and we assume their autocorrelation function $R_{n_{ij}}$ is the delta function, i.e. $R_{n_{ij}}(\tau) = 0$ for $\tau \neq 0$. Thus all the noise samples are un-correlated. Furthermore, n_{ij} are independent for j=0,1,2..N-1. Thus

$$E[(x'_i)^2] = E[(A_2 \cos(w_2(i\tau) + \phi_2) + \frac{1}{N}\sum_{j=0}^{N-1} n_{ij})^2]$$

$$= E[A_2^2 \cos^2(w_2 i\tau + \phi_2) + 2A_2 \cos(w_2 i\tau + \phi_2)\frac{1}{N}\sum_{j=0}^{N-1} n_{ij} + (\frac{1}{N}\sum_{j=0}^{N-1} n_{ij})^2]$$

$$= \mu^2 + \frac{1}{N^2}\sum_{j=0}^{N-1} E[n_{ij}^2] = \mu^2 + \frac{\sigma^2}{N} \tag{3.29}$$

Then

$$\sigma_e^2 = Var(x_i') = E[(x'_i)^2] - (E[x'_i])$$

$$= \mu^2 + \frac{\sigma^2}{N} - \mu^2 \quad = \frac{\sigma^2}{N} \tag{3.30}$$

So we get $P_{noise} = \sigma_e^2 = \frac{\sigma^2}{N}$.

Finally, the SNR is given as

$$SNR = \frac{P_{signal}}{P_{noise}} = \frac{A_2^2/2}{\sigma^2/N} = \frac{NA_2^2}{2\sigma^2} \tag{3.31}$$

Thus, using our approach, the performance can be improved as we take more samples. Specifically, under the same amplitude and noise condition, the SNR will increase N times, where N is the number of samples.

41

3.2.3 Simulation results under noisy environment

All the parameters for the simulation in this section are the same as table 2.1. In the following, we perform the simulation of detecting $s_2(t)$ under noisy environment.

A. Detection of $s_2(t)$

Figure 3.5 shows Amplitude Error Ratio under the SNR from -5~ 31 (dB). Next, we test the simulation with another case that $A_2(t)$ is the same as Eq. (2.52). The simulation results are shown in Figure 3.6. Obviously, the error ratio is smaller when SNR is higher. Note that each point in the figure is the average of 1000 simulations.
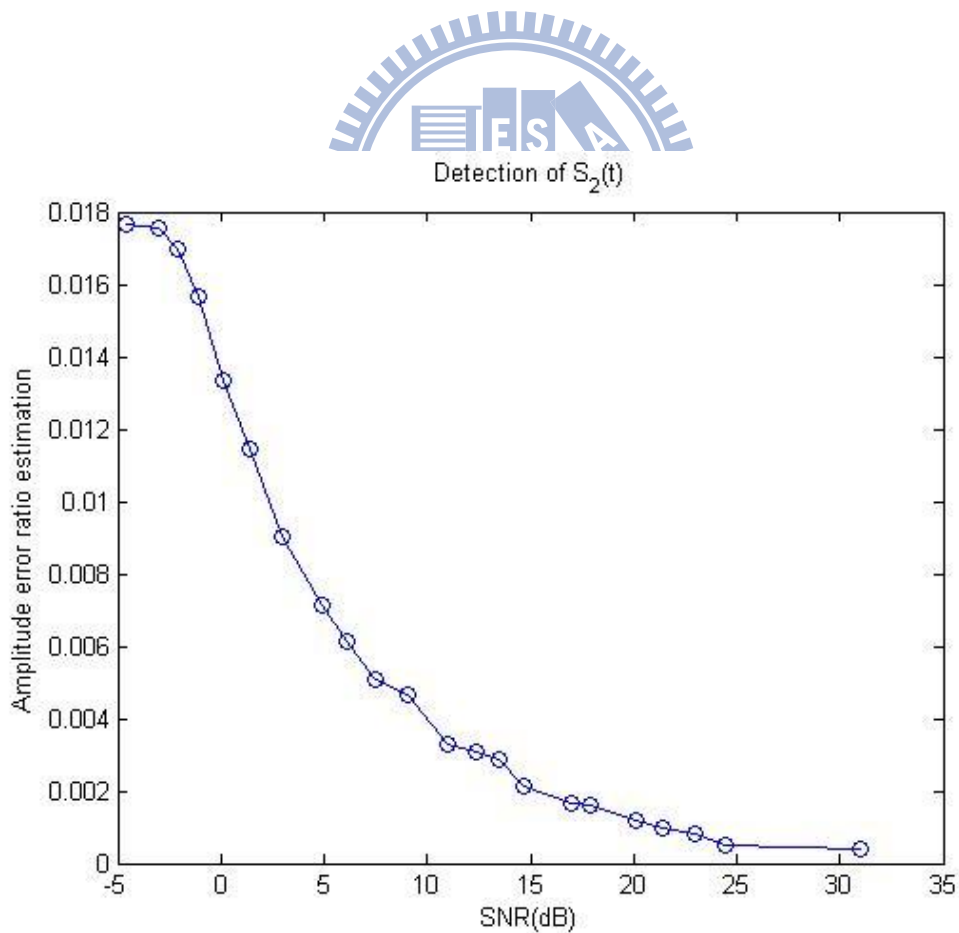
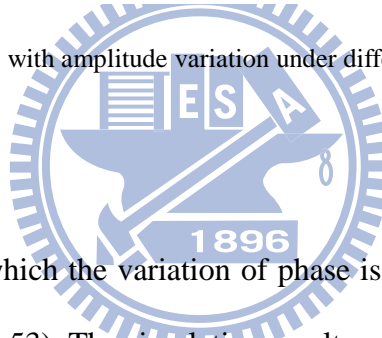Figure 3.5: Amplitude Error Ratio under different SNR and $A_2 / A_1 =1$.
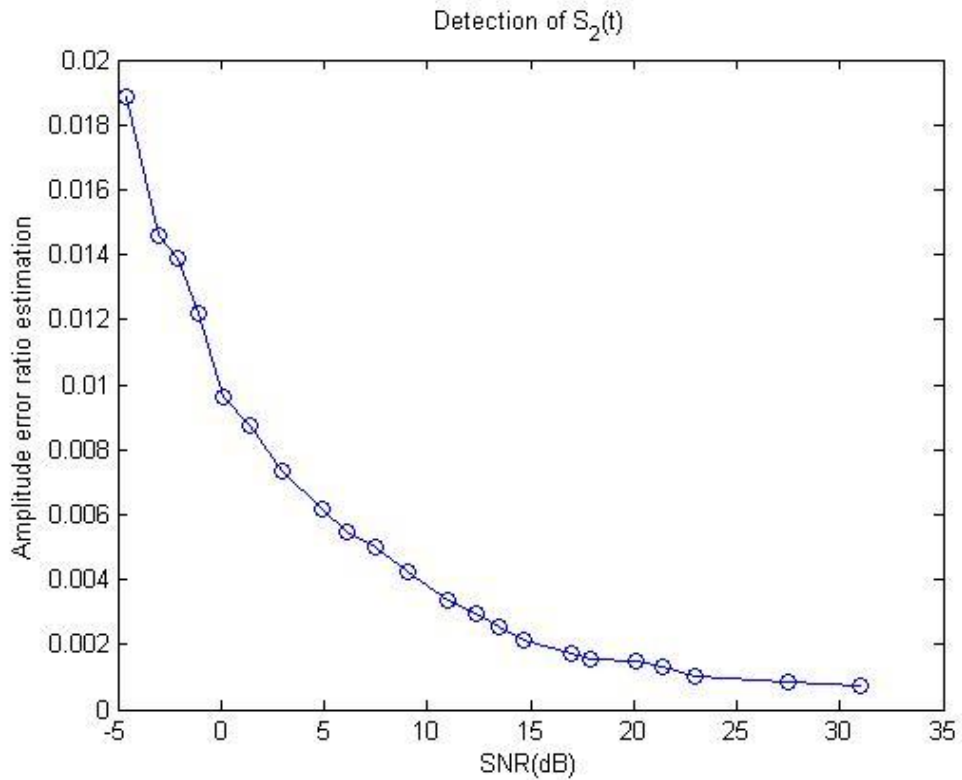
Figure 3.6: Amplitude Error Ratio with amplitude variation under different SNR and p=0.5 , T=4x10^{-5} .

We simulate the situation in which the variation of phase is random. We assume $\phi_{2,i}$ in the time interval $iT_{ob} \le t \le (i+1)T_{ob}$ as Eq. (2.53). The simulation results are shown in Figure 3.7 and Figure 3.8. The Amplitude Error Ratio is acceptable under this case, but Phase Shift Error Ratio is high at low SNR. It presents that the detection of phase variation is more sensitive to noise effect.

Detection of $S_2(t)$ with Phase shift=20(degree)
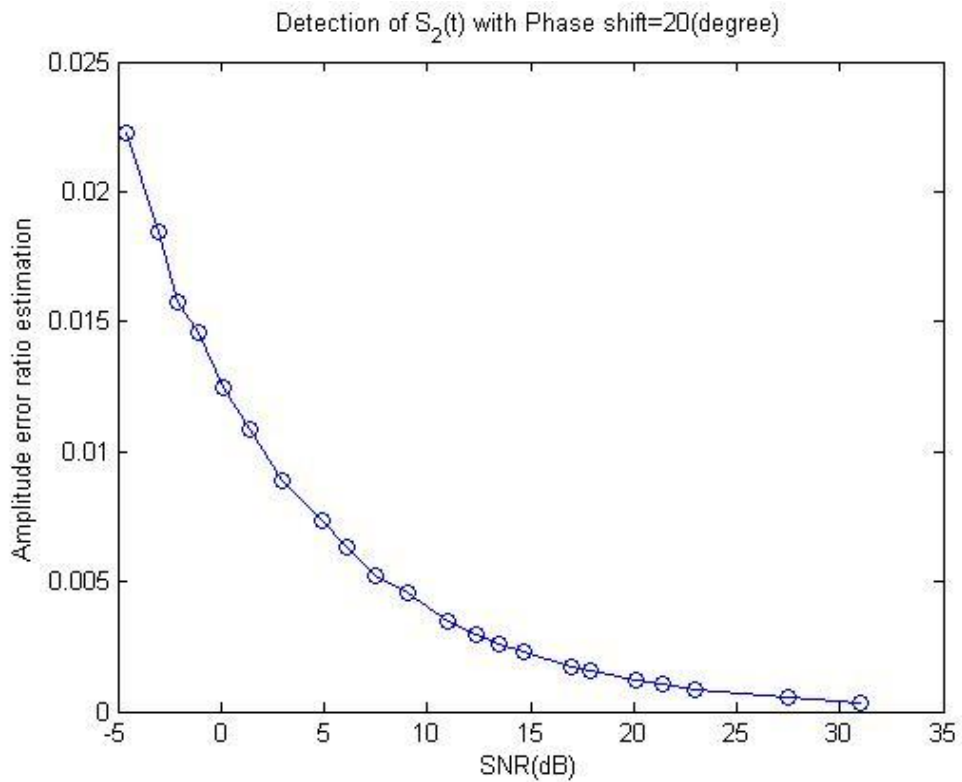
Figure 3.7: Amplitude Error Ratio with phase variation under different SNR.
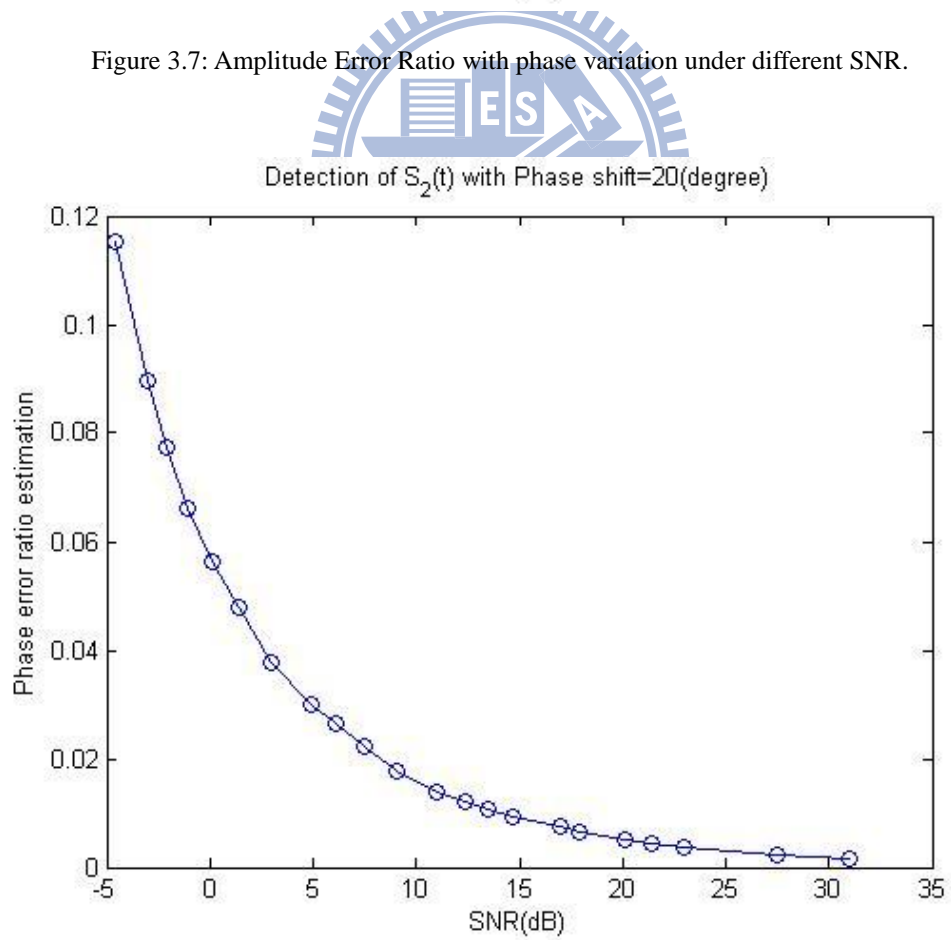
Detection of $S_2(t)$ with Phase shift=20(degree)

Figure 3.8: Phase Shift Error Ratio with phase variation under different SNR.

In the following, we combine the amplitude and phase variation under noisy environment in the simulation. The results are shown in Figure 3.9 and Figure 3.10. We find that the phase shift error reaches 3° when SNR= -5(dB). The amplitude and phase variation have larger effect on the accuracy of detection algorithm under noisy environment.
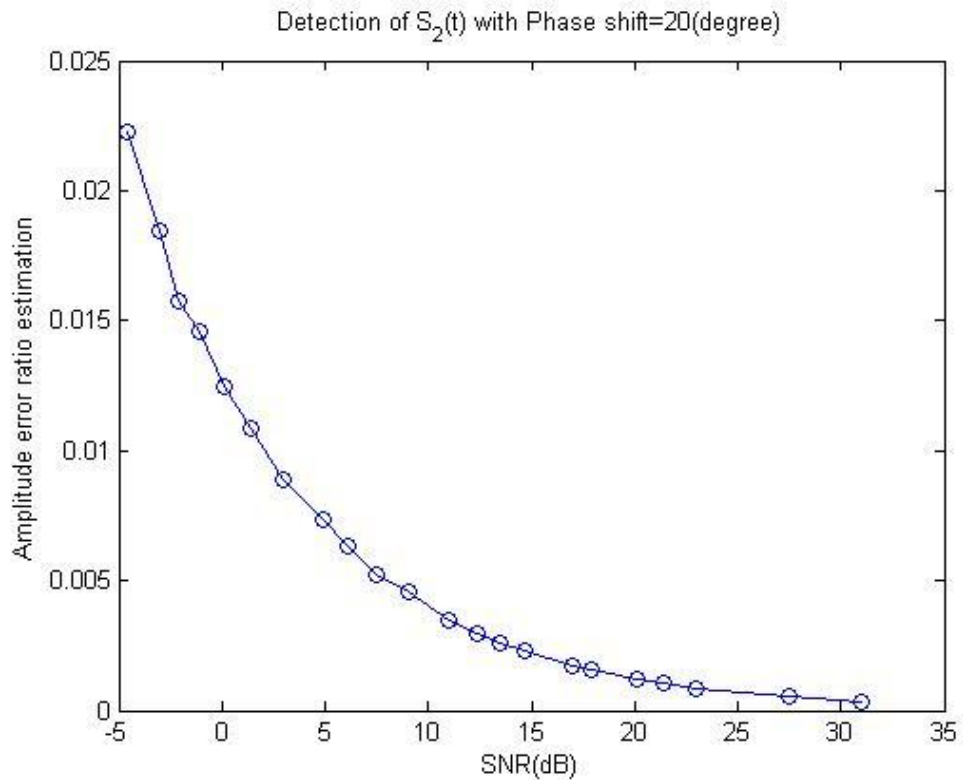

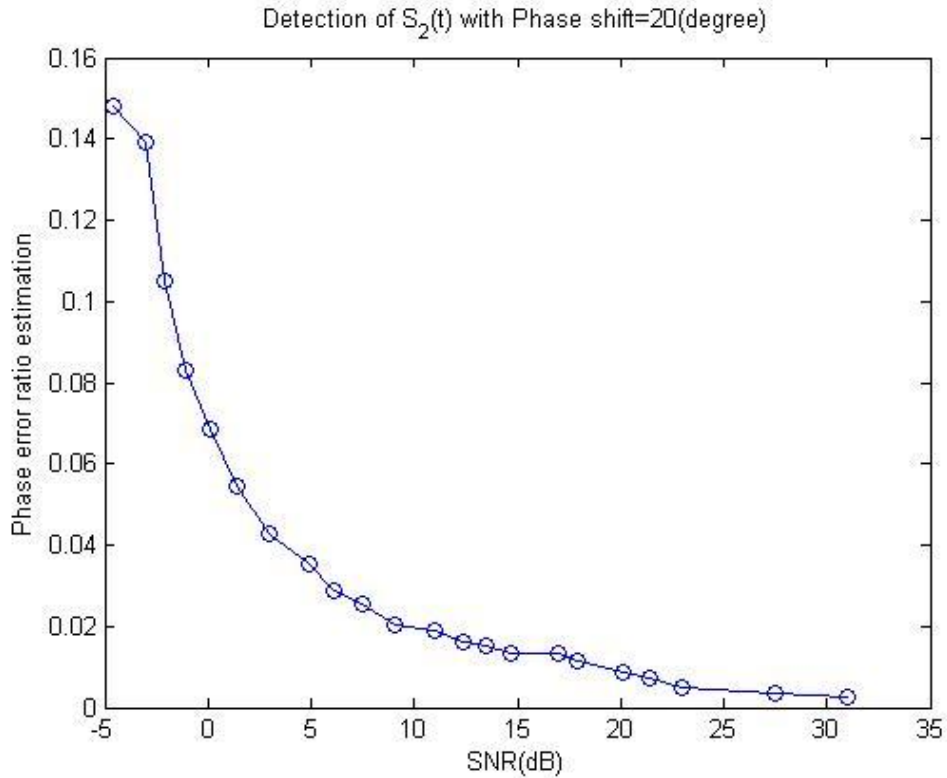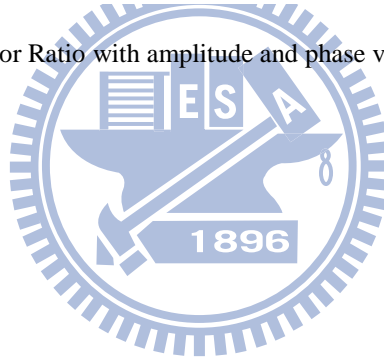Figure 3.9: Amplitude Error Ratio with amplitude and phase variation under different SNR.

Figure 3.10: Phase Shift Error Ratio with amplitude and phase variation under different SNR.

B. Detection of $s_1(t)$

We will follow the same steps as the simulation of detection of $s_2(t)$. Note the parameters of the simulation in this section are the same as table 2.2.

Figure 3.11 shows the Amplitude Error Ratio with amplitude variation under different SNR, where p=0.5 and T=4x10^{-5}. The Amplitude Error Ratio with phase variation under different SNR is shown in Figure 3.12, and the Phase Shift Error Ratio is shown in Figure 3.13, where the phase shift is 20°. We find the Phase Shift Error Ratio rises with phase variation, especially at low SNR. All the performances above are acceptable and reasonable. The error ratio gradually decreases when SNR increase.
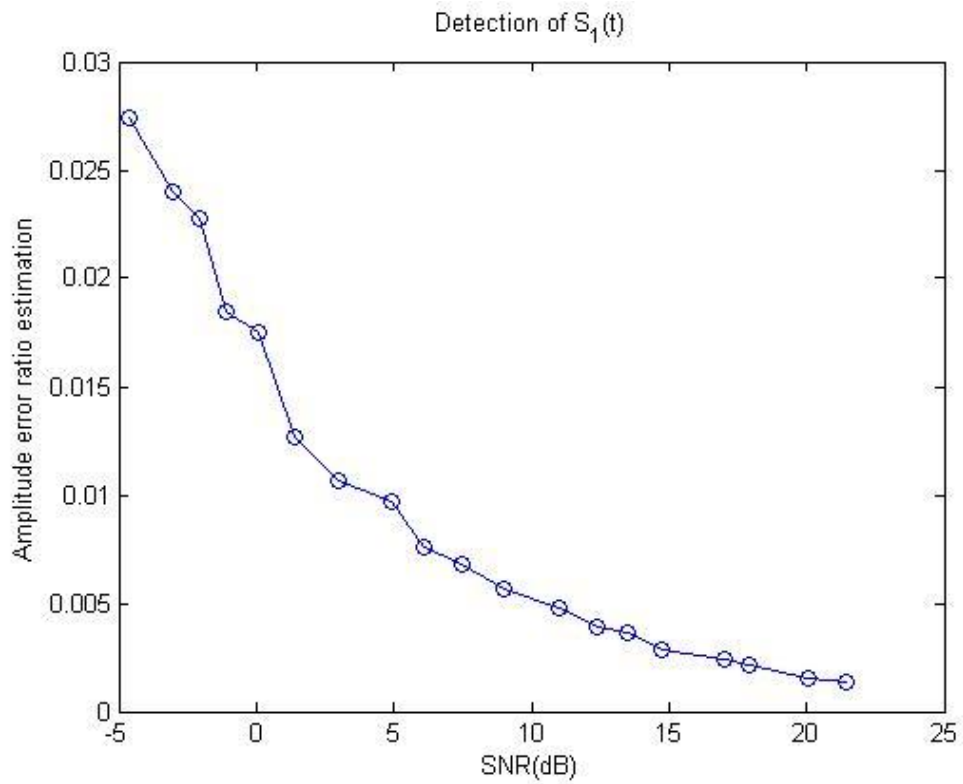
Figure 3.11: Amplitude Error Ratio with amplitude variation under different SNR and p=0.5 , T=4x10^{-5} .
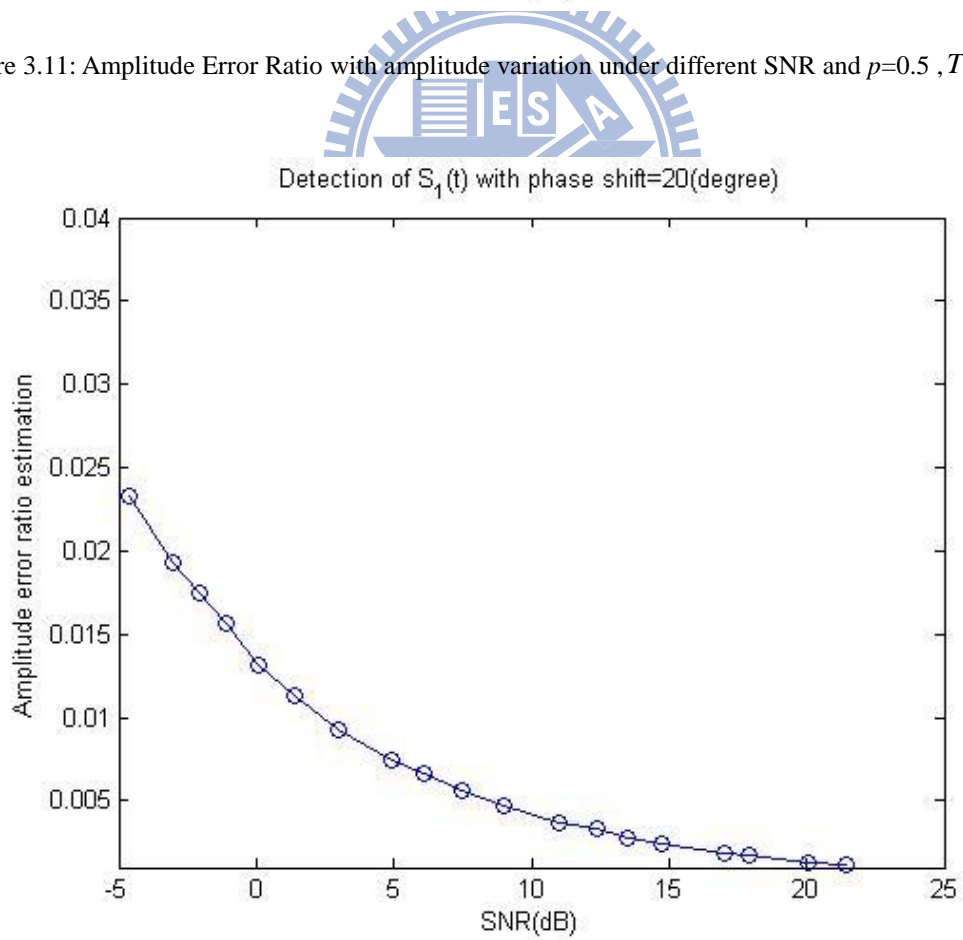

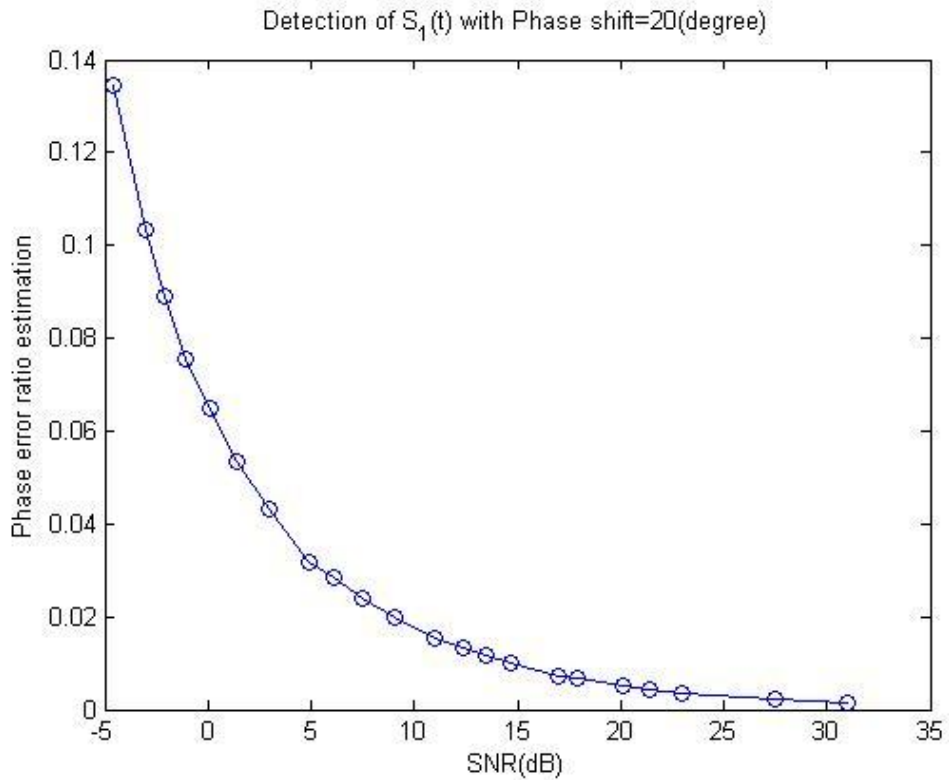Figure 3.12: Amplitude Error Ratio with phase variation under different SNR.

Figure 3.13: Phase Shift Error Ratio with phase variation under different SNR.

Next we will combine amplitude and phase variations to test our detection algorithm. The simulation results are shown in Figure 3.14 and Figure 3.15. Obviously, in this complex situation, the Amplitude Error Ratio and Phase Shift Error Ratio will rise.
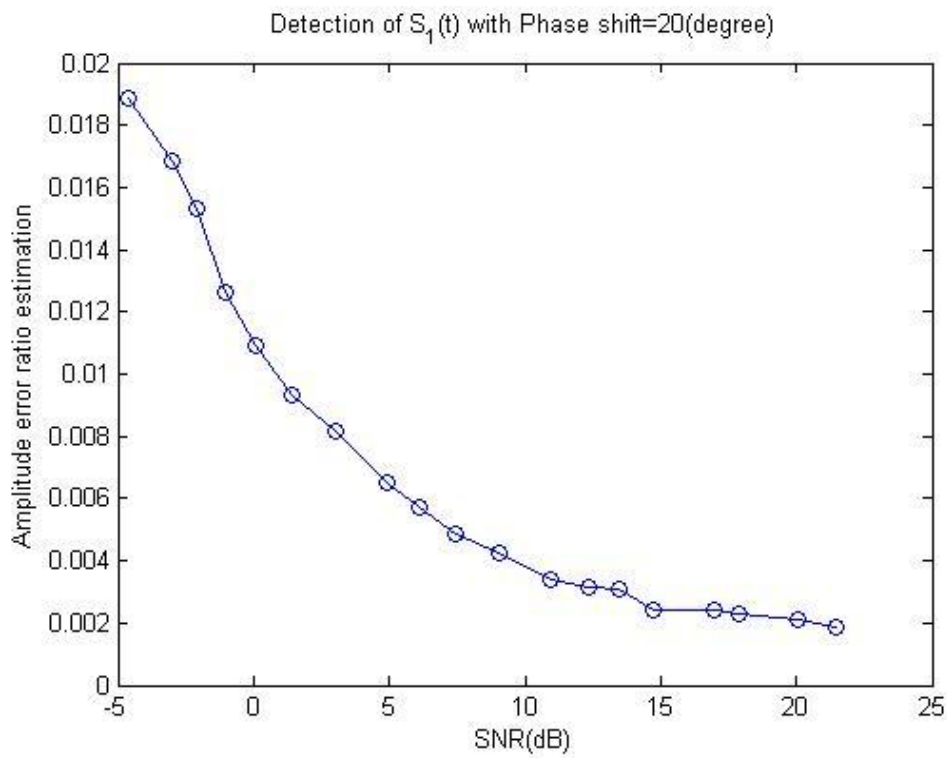
Figure 3.14: Amplitude Error Ratio with amplitude and phase variations under different SNR.
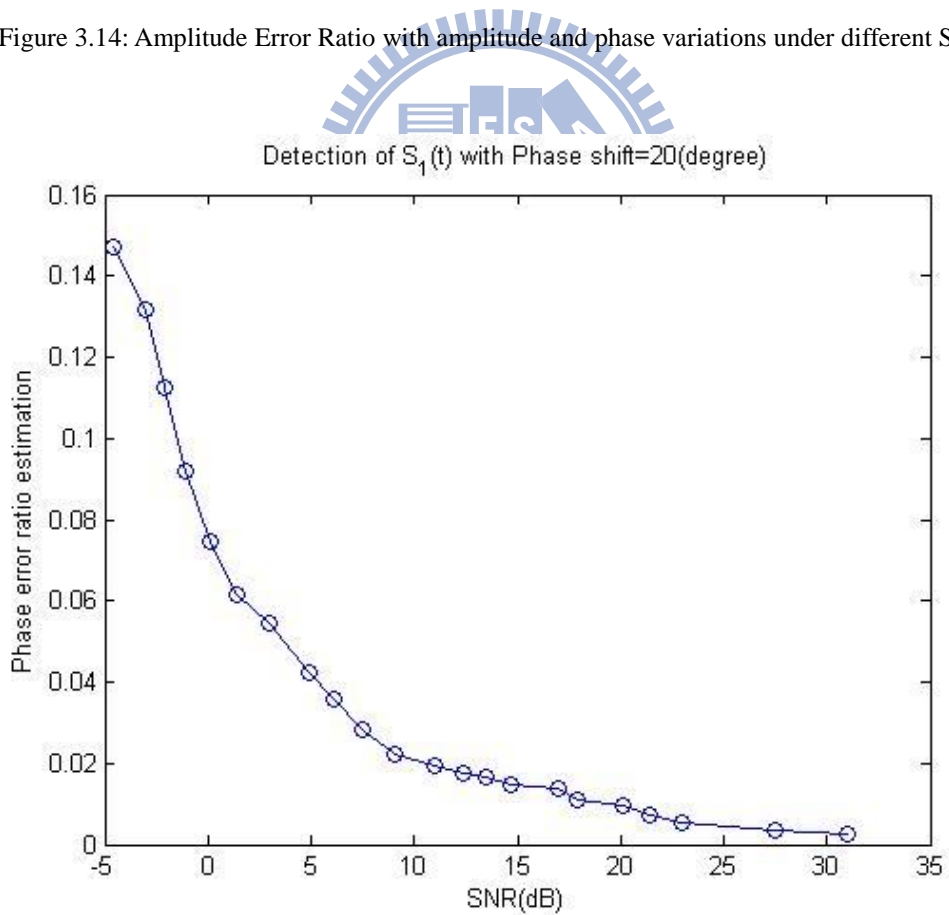

Figure 3.15: Phase Shift Error Ratio with amplitude and phase variations under different SNR.

C. Simulation with frequency offset under noisy environment

In section 3.1.3 the simulation results are under noiseless condition with frequency offsets. Now we will test the simulation of detecting $s_2(t)$ under noisy condition. First, we will perform the simulation with frequency offset Δf_1 (f_1 =610 MHz and phase shift=20°) under two SNR (SNR= 20 and 10 dB). Thus, the frequency offset Δf_1 ranges from 61 Hz to 61 KHz. The simulation results are shown in Figure 3.16 and Figure 3.17. The Amplitude Error Ratio is around 10^{-3} at SNR= 20 dB and 10 dB. But The Phase Error Ratio is around $10^{-1} \sim 10^{-2}$ at SNR= 20 dB and 10 dB.
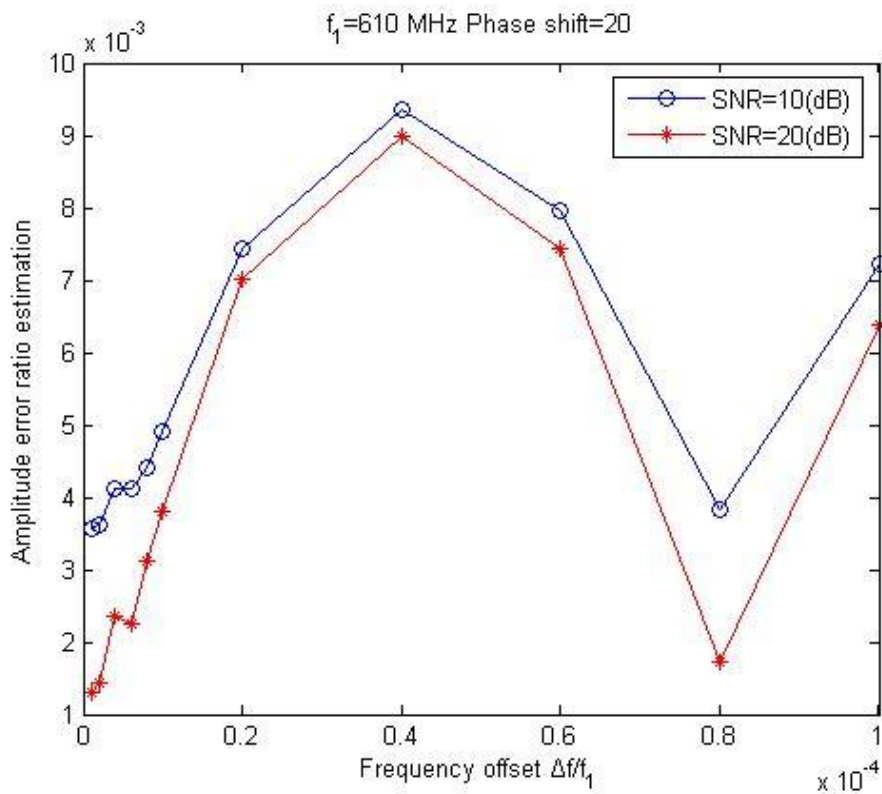

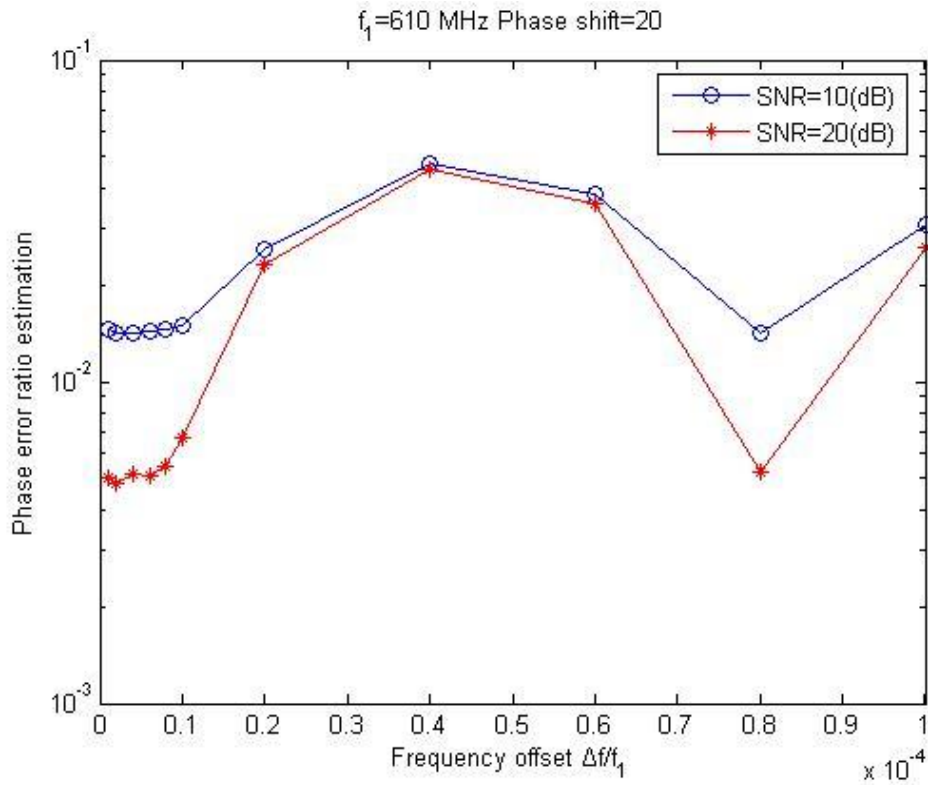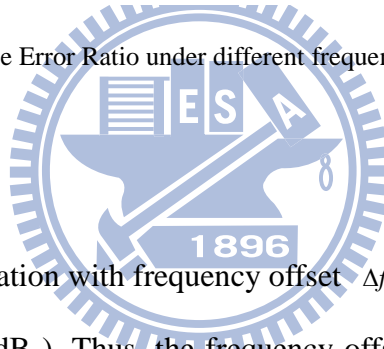Figure 3.16: Amplitude Error Ratio under different frequency offset $\Delta f_1 / f_1$.

Figure 3.17: Phase Error Ratio under different frequency offset $\Delta f_1 / f_1$.

Next, we will present the simulation with frequency offset Δf_2 (f_2 =609 MHz and phase shift=20°) under two SNR (SNR= 20 and 10 dB). Thus, the frequency offset Δf_2 ranges from 60.9 Hz to 60.9 KHz. The simulation results are shown in Figure 3.18 and Figure 3.19. The Amplitude Error Ratio is around $10^{-2} \sim 10^{-1}$ at SNR= 20 dB and 10 dB. The Phase Error Ratio is near $10^{-1} \sim 2$ at SNR= 20 dB and 10 dB. The two error ratios increase as Δf_2 rises from 60.9 Hz to 60.9 KHz, The Phase Error Ratio especially. And the maximum phase shift error reaches over 40°. It can be seen that the detection of $s_2(t)$ is more sensitive to frequency offset Δf_2 than frequency offset Δf_1 .
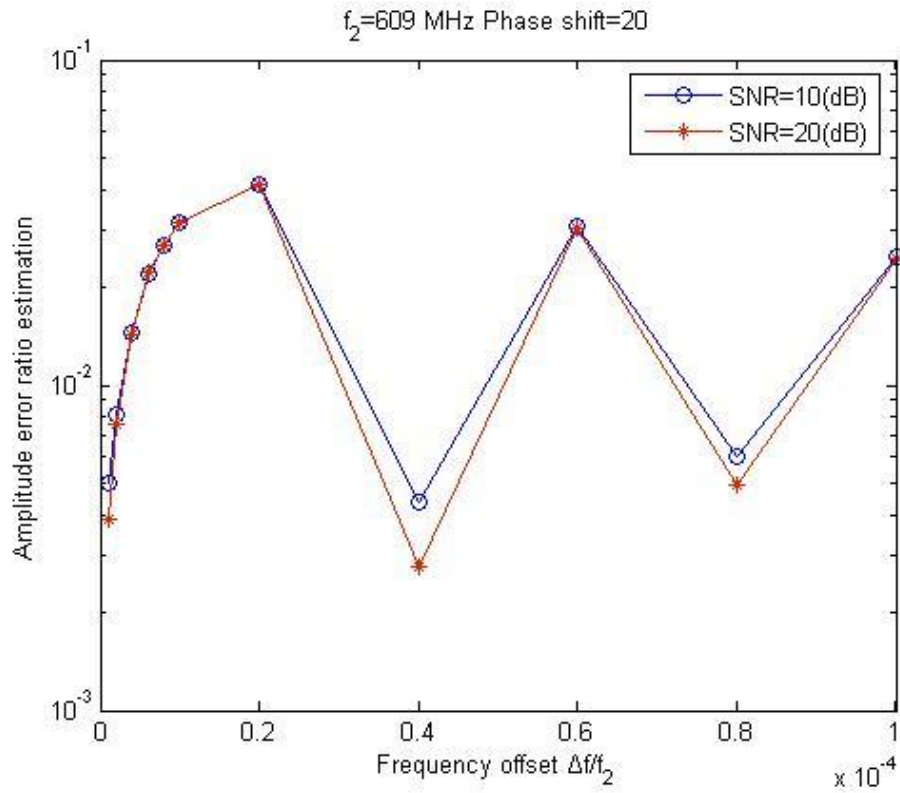
Figure 3.18: Amplitude Error Ratio under different frequency offset $\Delta f_2 / f_2$.
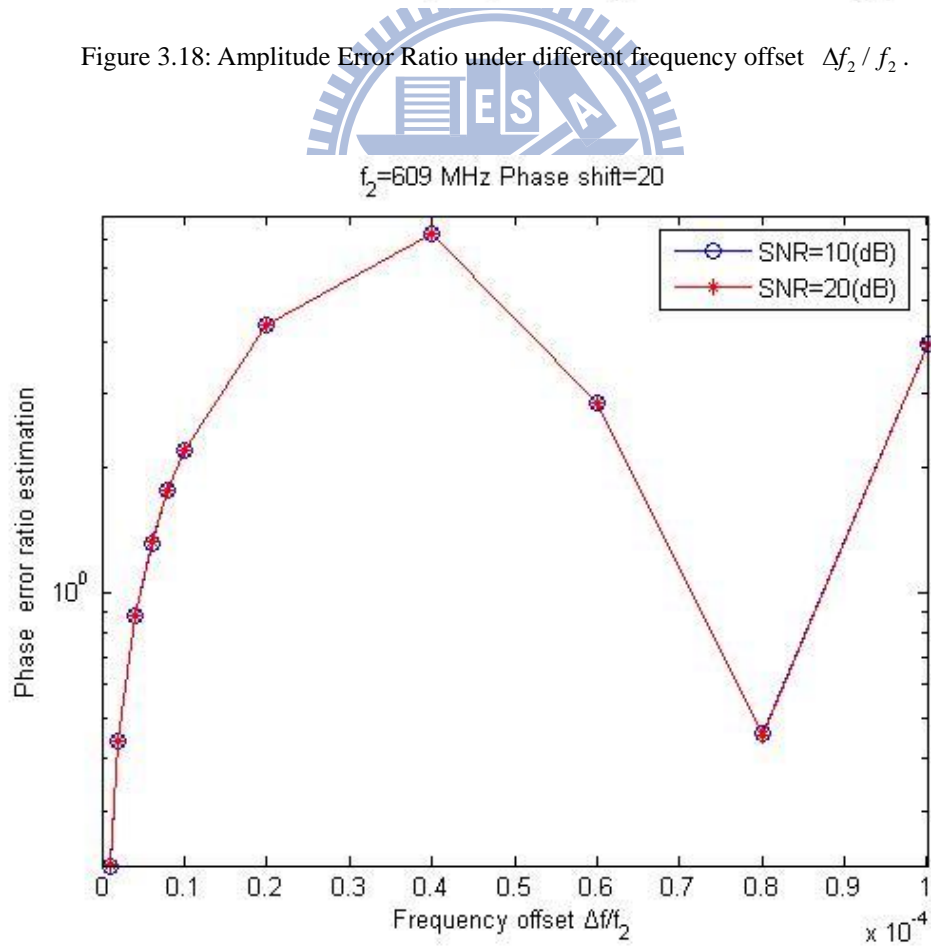
Figure 3.19: Phase Error Ratio under different frequency offset $\Delta f_2 / f_2$.

3.3 Summary

In this chapter, we analyzed the detection algorithm with two different effects: frequency offset effect, noise effect. We ran simulations with these two effects respectively, and then a combination of the two. These effects appear in any communication system in practice and affect the accuracy of our algorithm. It can be shown that our algorithm works in all conditions except for large frequency offset ($\Delta f > 609$ Hz) at SNR= 20 dB. The error performance can's be improved in that case even if increasing SNR.
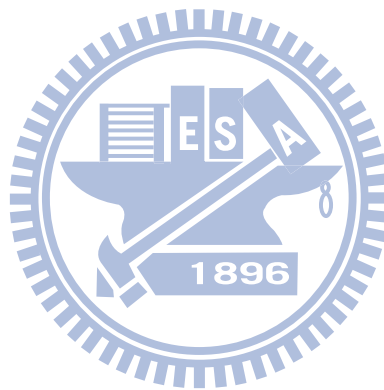
Chapter 4

Conclusions

In this thesis, we develop an algorithm to estimate the parameters of two closely spaced sinusoid signals. In Chapter 2, we describe in detail the detection algorithm. Our method, based on a simple sampling technique and statistic concepts, is able to detect two closely spaced sinusoid signals without mutual interference under ideal condition. The simulation results show that the detection of $s_2(t)$ is more sensitive to amplitude variation than phase variation under noiseless, and better performance is obtained in detecting $s_2(t)$ compared to $s_1(t)$ due to more sampling number. All the simulation results show that the algorithm work well under ideal situation.

In Chapter 3, we analyze detail performance of our algorithm with frequency offset effect and noise effect. The frequency offset Δf_2 ranges from 60.9 Hz to 60.9 KHz, and we add AWGN to the input signal for SNR ranging from 20 dB to 10 dB. It shows that the detecting $s_2(t)$ is more sensitive to frequency offset Δf_2 than frequency offset Δf_1. In addition, the error performance is not acceptable when frequency offset $\Delta f_2 > 609$ Hz at SNR= 20 dB.

To sum up, we successfully estimated the parameters of two closely spaced sinusoid signals without complex calculations, thus low cost for receivers. The frequency difference of two signals we set was 1 MHz in our simulation. In the future, we will continue to analyze the range of the frequency difference of two signals and further improve our algorithm to accommodate large frequency offset and noise.

References

[1]   C. J. Ying, L. C. Potter and R. L. Moses, "On model order determination for complex exponential signals: Performance of an FFT-initialized ML algorithm", Proc. 7th SP Workshop on Statistical Signal and Array Processing, Quebec, Canada, 26-29 June 1994, pp. 43-46.

[2]   J. Rissanen, "Modelling by shortest data description", *Automatica,* Vol. 14, 1978, pp. 465-471.

[3]   Y. Bresler and A. Macovski, "Exact maximum likelihood parameter estimation of superimposed exponential signals in noise," *IEEE Trans. Acoust., Speech and Signal Processing*, vol. ASSP-34, n. 5, pp. 1081-1089, Oct. 1986.

[4]   P. Stoica, R. L. Moses, B. Friedlander and T. Söderström, "Maximum Likelihood estimation of the parameters of multiple sinusoids from noisy measurements," *IEEE Trans. Acoust., Speech and Signal Processing*, vol. 37, n. 3, pp. 378-391, March 1989.

[5]   P. Stoica, P. Händel, T. Söderström, "Approximate maximum likelihood frequency estimation," *Automatica*, vol. 30, no. 1, pp. 131 - 145, January 1994.

[6]   M. D. Macleod, "Joint detection and high resolution ML estimation of multiple sinusoids in noise," in *Proc. of 2001 IEEE International Conference on Acoustics, Speech, and Signal Processing (ICASSP)*, Vol. 5, pp. 3065 - 3068, Salt Lake City, May 2001.